Linearity-Generating Processes, Unspanned Stochastic Volatility, and Interest-Rate Option Pricing

Peter Carr

Bloomberg LP and Courant Institute, New York University

Xavier Gabaix

Stern School of Business, New York University

Liuren Wu

Zicklin School of Business, Baruch College, CUNY

ABSTRACT

We propose to use the linearity-generating framework to accommodate the evidence of unspanned stochastic volatility: Variations in implied volatilities on interest-rate options such as caps and swaptions are independent of the variations on the interest rate term structure. Under this framework, bond valuation depends only on the transition dynamics of interest-rate factors, but not on their volatilities. Thus, interest-rate volatility is truly unspanned. Furthermore, this framework allows tractable pricing of options on any bond portfolios, including both caps and swaptions. This feat is not possible under existing exponential-affine or quadratic frameworks. Finally, the framework allows sequential estimation of the interest-rate term structure and the interest-rate option implied volatility surface, thus facilitating joint empirical analysis. Within this framework, we perform specification analysis on interest-rate factor transition dynamics and its relation to the interest-rate term structure; we also analyze the interest-rate volatility dynamics and its impact on interest-rate option pricing. We estimate several specifications for the transition dynamics to ten years worth of U.S. dollar LIBOR and swap rates across 15 maturities. We also estimate several interest-rate volatility dynamics specifications using ten years of swaption implied volatilities across a matrix of ten option maturities and seven swap tenors. The estimation results show that the volatility dynamics dictate the option implied volatility variation along the option maturity dimension, whereas the interest-rate transition dynamics dictate the implied volatility variation along the underlying swap maturity dimension.

JEL Classification: C13; C51; G12; G13.

Keywords: Linearity-generating processes, stochastic discount factors, swaptions, unspanned volatility.

Very preliminary. We thank David Backus, Stanley Zin for comments. We welcome comments, including references that we have inadvertently missed. Peter Carr is at Bloomberg LP and Courant Institute, New York University, 731 Lexington Avenue, New York, NY 10022; tel: (212) 893-5056; fax: (917) 369-5629; email: pcarr4@bloomberg.com. Xavier Gabaix is at Stern School of Business, New York University, 44 West 4th Street, New York, NY 10012; tel: (212) 998-0257; fax: (212) 995-4233; email: xgabaix@stern.nyu.edu. Liuren Wu is at Zicklin School of Business, Baruch College, One Bernard Baruch Way, Box B10-225, New York, NY 10010; tel: (646) 312-3509; fax: (646) 312-3451; email: Liuren_Wu@baruch.cuny.edu. Gabaix thanks the NSF for support.

Under classic one-factor interest-rate models such as Vasicek (1977) or Cox, Ingersoll, and Ross (1985), the different parts of the interest-rate term structure are tightly linked to the short-term interest rate dynamics under the so-called risk-neutral measure. The short rate level determines the short end of the yield curve, the risk-neutral mean of the short rate determines the long end of the yield curve. The speed with which shocks to the short rate transmit to long rates is controlled by the risk-neutral mean reversion speed of the short rate. Finally, the curvature of the yield curve is determined by the short rate volatility.

During the past decade, term structure modeling with multi-dimensional risk structures has developed rapidly. Prominent examples include the exponential affine class of Duffie, Pan, and Singleton (2000), under which zero-coupon bond prices are exponential affine in the state vector, and the exponential quadratic class of Leippold and Wu (2003), where zero-coupon bond prices are exponential quadratic functions of the state vector. Despite the rapid development and multi-dimensional extension, the simple intuition from the classic one factor models remains as the guiding yardstick in designing or explaining the different roles played by different interest-rate factors.

The intuition is challenged, however, when a few studies, e.g., Collin-Dufresne and Goldstein (2002) and Heidari and Wu (2003), find that a large proportion of the movements in the interest-rate option implied volatilities are independent of the factors identified from the yield curve, a phenomenon labeled as "unspanned stochastic volatility." At-the-money option implied volatilities approximate well the risk-neutral expected value of the underlying asset return volatility (Carr and Wu (2006)). Intuition from the classic models suggests that interest-rate volatility variation should show up on the yield curve as variation in the yield curve curvature. It is difficult to reconcile the independent movements with most existing modeling approaches, except under specific parametric constraints (Collin-Dufresne and Goldstein (2002)). Probably related to the unspanned volatility phenomenon, researchers have found that dynamic term structure models that price the term structure well generate very poor performance in pricing and hedging interest-rate options (Dai and Singleton (2003), Li and Zhao (2006), and Heidari and Wu (2008)).

Most recently, Gabaix (2007) develops a new class of asset pricing models, under which bond prices are linear in a set of yield curve factors. This linearity feature has profound implications that are drastically different from the above-discussed classic models. In particular, the linear relation between bond prices and the yield curve factors dictates that only the risk-neutral drift, or the transition dynamics, of the interest-rate

factors enter the bond pricing equation but that neither volatilities of these factors nor the volatility dynamics affect bond pricing. Therefore, if these factors show stochastic volatility, these stochastic volatilities are truly unspanned and completely un-identified from the yield curve.

Another important implication of the linear structure is that both coupon bonds and swap rates are also linear in the state vector. If one can price an option on a zero-coupon bond, pricing an option on a coupon bond or a swap is equally tractable. This is not the case for the exponential affine or quadratic class. Researchers often resort to different dynamics specifications for pricing caps and floors, which are essentially options on zero-coupon bond, than for pricing swaptions; or one must resort to linear approximations to retain tractability (Heidari, Hirsa, and Madan (2007) and Schrager and Pelsser (2006)). By starting with a linearity-generating process, we remove the need for linear approximation on the pricing relation and circumvent the concern on internal consistency when different dynamics or different approximations are used to price different contracts.

Finally, the feature that interest-rate volatilities and their dynamics do not show up in bond pricing but show up in interest-rate options leads naturally to a two-step sequential estimation procedure, under which one can identify the interest-rate transition dynamics from the interest-rate term structure during the first step and then identify the interest-rate volatility dynamics from the interest-rate options during a second step. The sequential estimation breaks a large identification problem into smaller, manageable levels and thus facilitates a joint analysis of both interest-rate term structure and interest-rate options.

In this paper, we work within the linearity-generating framework and perform specification analysis on (i) the interest-rate factor transition dynamics and its relation to the interest-rate term structure, and (ii) the interest-rate volatility dynamics and its impact on interest-rate option pricing. Then, we estimate several specifications for the interest-rate factor transition dynamics using ten years worth of U.S. dollar LIBOR and swap rates across 15 maturities, and we also estimate several interest-rate volatility dynamics specifications using ten years of swaption implied volatilities across a matrix of ten option maturities and seven swap tenors. The sequential procedure and the large amount of data enables us to identify the transition and volatility dynamics accurately. The estimation results show that the volatility dynamics dictate the option implied volatility variation along the swaption maturity dimension, whereas the interest-rate transition dynamics dictate the implied volatility variation along the underlying swap maturity dimension.

The remaining of the paper is organized as follows. The next section performs specification analysis on the linearity-generating framework. We start with a one-factor example to illustrate the intuition and the general ideas, and then proceed to define an $(m+n)$ factor structure that includes an m-dimensional transition matrix to determine the interest-rate term structure and an n-dimensional stochastic volatility dynamics to govern the swaption implied volatility surface. We clarify the identification conditions under such a generic factor structure. Section 2 analyzes the data on LIBOR, swap rates, and swaption implied volatilities. Section 3 describes the two-step sequential estimation procedure for identifying the transition dynamics and volatility structures. Section 4 discusses the estimation results on the first-stage estimation and the interest-rate term structure variation. Section 5 analyzes the option pricing estimation results. Section 6 concludes.

1. Linearity-generating processes and unspanned volatility

We fix a filtered complete probability space $\{\Omega, \mathcal{F}, \mathbb{P}, (\mathcal{F}_t)_{0\leq t\leq \mathcal{T}}\}$ satisfying the usual technical conditions with $\mathcal{T}$ being some finite, fixed time. For any time $t \in [0,\infty)$ and an expiry date $T \geq t$, we use $P(t,T)$ to denote the time-t value of a zero-coupon bond with time-to-maturity $\tau = T-t$. The instantaneous interest rate, or the short rate, r, is defined by continuity:

$$r_t \equiv \lim_{T\downarrow t} \frac{-\ln P(t,T)}{T-t}. \tag{1}$$

We assume no arbitrage in the economy. Then, under certain technical conditions, there exists at least one strictly positive stochastic process M_t, which we call the *state price deflator*, such that the deflated gains process associated with any admissible trading strategy is a martingale (Cochrane (2004), Duffie (1992), Harrison and Kreps (1979)). In particular, time-t fair value of a claim to a terminal payoff Π_T at time $T > t$ can be written as

$$V(t,T) = \mathbb{E}_t\left[\frac{M_T}{M_t}\Pi_T\right], \tag{2}$$

where $\mathbb{E}_t[\cdot]$ denotes the expectation operator conditional on filtration $\mathcal{F}_t$ and under measure $\mathbb{P}$.

This stochastic process M_t is unique when the market is complete. The ratio of M at two time horizons $M_{t,T} = M_T/M_t$ is referred to as the stochastic discount factor or the pricing kernel. The state price deflator is related to the instantaneous interest rate by

$$dM_t/M_t = -r_t dt - \gamma(Z)^\top dZ_t, \tag{3}$$

where Z_t represents the risk sources of the economy and $\gamma(Z_t)$ measures the market prices of these economic risks. We can also write the state price deflator via the following multiplicative decomposition,

$$M_t = M_0 \exp\left(-\int_0^t r_s ds\right) \mathcal{E}\left(-\int_0^t \gamma(Z_s) dZ_s\right), \tag{4}$$

where $\mathcal{E}(\cdot)$ denotes the stochastic exponential martingale operator (Jacod and Shiryaev (1987) and Rogers and Williams (1987)). The exponential martingale defines the Radon-Nikodým derivative that transforms the statistical measure $\mathbb{P}$ to the risk-neutral measure $\mathbb{Q}$, under which the contingent claim valuation can be written as,

$$V(t,T) = \mathbb{E}_t^{\mathbb{Q}}\left[\exp\left(-\int_t^T r_s ds\right)\Pi_T\right]. \tag{5}$$

In what follows, we first use a one-factor example to illustrate the intuition and the general idea behind the linearity-generating framework. We then perform specification analysis on (i) the interest-rate transition dynamics and the impact on bond pricing and (ii) the interest-rate volatility dynamics and the effect on option pricing.

1.1. A one-factor example

Let $r_t = \theta_r + x_t$, with θ_r being the long-run risk-neutral mean of the short rate and x_t denoting a zero-mean random process that captures the short rate gap from its long-run mean. Gabaix (2007) proposes the following $\mathbb{Q}$-dynamics for x_t,

$$dx_t = -x_t(\kappa - x_t)dt + dn_t \tag{6}$$

where n_t denotes the martingale component. Under this dynamics specification, the value of the zero-coupon bond $P(t,T)$ is affine in x_t,

$$P(t,T) = \mathbb{E}_t^{\mathbb{Q}}\left[\exp\left(-\int_t^T r_s ds\right)\right] = e^{-\theta_r \tau}\left(1 - \frac{1-e^{-\kappa\tau}}{\kappa} x_t\right), \quad \tau = T-t. \tag{7}$$

The bond value depends on the long-run mean of the short rate θ_r, the drift coefficient κ that controls the transition dynamics of the short rate, and the current level of short-rate gap x_t. However, the pricing equation does not depends on the specification of the martingale component n_t and hence does not depend on the interest-rate volatility dynamics.

The linear pricing structure in equation (7) has important implications. First, even if the short rate shows stochastic volatility, its variation will not show up in the term structure of interest rates. In this sense, the interest-rate volatility is truly unspanned by the interest-rate term structure, a phenomenon that has been documented empirically by Collin-Dufresne and Goldstein (2002), Heidari and Wu (2003), Li and Zhao (2006), and Heidari and Wu (2008). Second, the linear structure also suggests that all simply compounded rates and all coupon bonds are also linear in the short-rate gap factor x_t.

It is also helpful to consider an alternative representation of the economy,

$$Y_t = \begin{pmatrix} 1 - \frac{x_t}{\kappa} \\ \frac{x_t}{\kappa} \end{pmatrix} M_t, \tag{8}$$

where M_t denotes the state price deflator. Then, we can show (in Appendix A) that the $\mathbb{P}$-dynamics of Y_t is governed by a diagonal transition matrix A,

$$\mathbb{E}_t\left[dY_t\right] = -AY_t dt, \quad \text{with} \quad A = \begin{pmatrix} \theta_r & 0 \\ 0 & \kappa + \theta_r \end{pmatrix}. \tag{9}$$

Hence, we can solve the conditional expectations of Y_T via the matrix exponential of the transition matrix,

$$\mathbb{E}_t\left[Y_T\right] = e^{-A\tau} Y_t = e^{-\theta_r \tau} \begin{pmatrix} 1 - \frac{x_t}{\kappa} \\ e^{-\kappa\tau}\frac{x_t}{\kappa} \end{pmatrix} M_t. \tag{10}$$

Furthermore, we can write the state price deflator as $M_t = \nu^\top Y_t$, with $\nu^\top = (1,1)$. Thus, using the result in (10), we can derive the zero-coupon bond prices directly by taking expectations on the pricing kernel under the statistical measure $\mathbb{P}$,

$$P(t,T) = \mathbb{E}_t\left[\frac{M_T}{M_t}\right] = \frac{1}{M_t}\mathbb{E}_t\left[\nu' Y_T\right] = \frac{1}{M_t}\nu' e^{-A\tau} Y_t = e^{-\theta_r \tau}\left(1 - \frac{1-e^{-\kappa\tau}}{\kappa} x_t\right), \tag{11}$$

which is identical to the bond pricing solution in (7).

Although the martingale component does not affect the bond pricing equation, it does affect the pricing of interest-rate options. To price interest-rate options tractably, instead of directly specifying the martingale component in the short rate dynamics, we start with specifications on the innovation of the transformed vector Y_t. One simple specification can be,

$$Y_t = e^{-\theta_r t}\begin{pmatrix} \alpha_0 + \beta_0 Z_t \\ e^{-\kappa t}\left(\alpha_1 + \beta_1 Z_t\right) \end{pmatrix}, \tag{12}$$

where $(\alpha_0, \alpha_1, \beta_0, \beta_1)$ are scaling coefficients and Z_t denotes a non-negative martingale starting at $Z_0 = 1$. With this specification, we have the state price deflator as,

$$M_t = \nu' Y_t = e^{-\theta_r t}\left(\alpha_0 + \beta_0 Z_t + e^{-\kappa t}\left(\alpha_1 + \beta_1 Z_t\right)\right), \tag{13}$$

and in the form of stochastic differential equation,

$$dM_t / M_t = -r_t dt - \gamma(Z_t) dZ_t, \tag{14}$$

where the market price of Z risk is given by

$$\gamma(Z) = -\frac{(\beta_0 + e^{-\kappa t}\beta_1)}{(\alpha_0 + \beta_0 Z_t) + e^{-\kappa t}\left(\alpha_1 + \beta_1 Z_t\right)}. \tag{15}$$

To guarantee the positivity of the deflator for all t, we constraint $\alpha_0 > 0, \beta_0 \geq 0, \beta_1 \geq 0$, $\alpha_0 + \alpha_1 \geq 0$. Hence, the market price of risk is negative.

From (13), we can derive the zero-coupon bond value as,

$$\begin{aligned} P(t,T) &= \mathbb{E}_t\left[\frac{M_T}{M_t}\right] = \frac{1}{M_t}e^{-\theta_r T}\left(\alpha_0+\beta_0 Z_t + e^{-\kappa T}(\alpha_1+\beta_1 Z_t)\right) \\ &= e^{-\theta_r \tau}\left(1-\frac{1-e^{\kappa\tau}}{\kappa}\frac{\kappa e^{-\kappa t}(\alpha_1+\beta_1 Z_t)}{\alpha_0+\beta_0 Z_t+e^{-\kappa t}(\alpha_1+\beta_1 Z_t)}\right). \end{aligned} \tag{16}$$

Comparing (7) with (16), we have x_t related to Z_t by

$$x_t = \frac{\kappa e^{-\kappa t}(\alpha_1+\beta_1 Z_t)}{\alpha_0+\beta_0 Z_t+e^{-\kappa t}(\alpha_1+\beta_1 Z_t)}. \tag{17}$$

Appendix A shows that the x_t dynamics is consistent with the specification in equation (6) under the risk-neutral measure $\mathbb{Q}$, with the martingale component given by

$$dn_t = \frac{(x_{\max}(t)-x_t)(x_t-x_{\min}(t))}{(x_{\max}(t)-x_{\min}(t))}\frac{dZ_t}{Z_t}, \tag{18}$$

where $x_{\max}$ and $x_{\min}$ define the maximum and minimum values for x_t,

$$x_{\max}(t) = \frac{\kappa e^{-\kappa t}\beta_1}{\beta_0+e^{-\kappa t}\beta_1}, \quad x_{\min}(t) = \frac{\kappa e^{-\kappa t}\alpha_1}{\alpha_0+e^{-\kappa t}\alpha_1}. \tag{19}$$

Thus, the volatility of x_t is parabolic and goes to zero at the two boundaries, $[x_{\min}(t), x_{\max}(t)]$.

Equation (16) derives the fair value of the zero-coupon bond as a function of the model parameters and the single factor x_t or Z_t. Observed bond prices can deviate from the fair values either due to model mis-specification or short-term market dislocations. Regardless the source, interest-rate options are written on observed bond prices or interest-rate quotes, not on model values. Hence, we need to explicitly adjust for the mismatch, if any, between the model values and observed market quotes. For this purpose, we follow Heath, Jarrow, and Morton (1992) and Hull and White (1990) to accommodate the currently observed yield curve through a deterministic time function. Specifically, we adjust the fair value of the state price deflator M_t by a multiplicative corrective term R_t, defined as

$$R_t = e^{-\int_0^t \rho_u du}. \tag{20}$$

Then, the observed zero-coupon bond prices can be written as

$$\widehat{P}(t,T) = \mathbb{E}_t\left[\frac{M_T R_T}{M_t R_t}\right] = P(t,T)e^{-\int_t^T \rho_u du} = P(t,T)R(t,T),$$

with $R(t,T) \equiv e^{-\int_t^T \rho_u du}$.

Now consider pricing European options on a portfolio of coupon bonds. The time-T observed price of a portfolio of bonds that pays coupon c_s at s for a finite collection of dates $s \geq T$ can be written as,

$$\widehat{P}_T = \sum_s c_s \widehat{P}(T,s) = \frac{1}{M_T}\sum_s c_s R(T,s)e^{-\theta_r s}\left[\alpha_0 + \beta_0 Z_T + e^{-\kappa s}(\alpha_1 + \beta_1 Z_T)\right]. \tag{21}$$

We consider a European option with expiration date T on the bond portfolio with the terminal payoff $\Pi_T = \left(D\widehat{P}_T - K\right)^+$. Its time-$t$ value can be written as $V_t = \mathbb{E}_t\left[M_T\left(D\widehat{P}_T - K\right)^+\right]/M_t$. The following proposition converts the European option on the bond portfolio to a European option on the non-negative martingale Z_T.

Proposition 1 *Under the linearity-generating dynamics specified in (12), we can write the present value of a European option on a portfolio of bonds as the forward value of a European option on the non-negative martingale Z_T. Specifically, the time-t value of an option with maturity T on a bond portfolio specified by (21) can be written as,*

$$V_t = \mathbb{E}_t\left[\frac{M_T}{M_t}\left(D\widehat{P}_T - K\right)^+\right] = \mathbb{E}_t\left[(F_t + G_t Z_T)^+\right] \tag{22}$$

where the deterministic coefficients F_t and G_t are given by

$$F_t = \frac{1}{M_t}\sum_s \eta_s R(T,s)e^{-\theta_r s}\left(\alpha_0 + e^{-\kappa s}\alpha_1\right), \quad G_t = \frac{1}{M_t}\sum_s \eta_s R(T,s)e^{-\theta_r s}\left(\beta_0 + e^{-\kappa s}\beta_1\right), \tag{23}$$

where $\eta_T = Dc_T - K$ and $\eta_s = Dc_s$ for $s > T$.

The proof follows readily by plugging in the expression for $\widehat{P}_T$ in (21) and collecting terms. The proposition can be applied to a wide range of actively traded interest-rate derivatives such as caps, floors, and swaptions, as they can all be written as European options on a portfolio of zero-coupon bonds.

Corollary 1 *If we assume that the innovation Z_t follows a geometric Brownian motion $Z_t = \exp\left(\sigma W_t - \sigma^2 t/2\right)$, we can represent the value of European options on a portfolio of bonds in the Black-Scholes formula,*

$$V_t = V_{Call}^{BS}\left(G_t Z_t, -F_t, \sigma\sqrt{T-t}\right) \tag{24}$$

where $V_{Call}^{BS}\left(S, K, \sigma\sqrt{T}\right)$ is the Black-Scholes value of a call with initial value S, strike K, volatility σ, maturity T, and interest rate 0.

Thus, tractable specifications on the Z_t dynamics generate tractable pricing of options on many actively traded interest-rate derivatives. In particular, while the specification of the interest-rate transition dynamics (κ) determines the bond pricing and hence the interest-rate term structure, it is the dynamics specification on the innovation Z_t that determines the variation of the option value.

1.2. The general ($m+n$) factor structure

In a generate set up, we consider an *m*-dimensional interest-rate term structure and *n*-dimensional independent interest-rate volatility factor structure, embedded in the following specification,

$$Y_t = e^{-At}\left(\alpha + \beta Z_t\right) = M_t X_t, \quad M_t = \nu^\top Y_t, \tag{25}$$

where the transition matrix $A \in \mathbb{R}^{(m+1)\times(m+1)}$ and the loading vector $\nu \in \mathbb{R}^{(m+1)}$ determine the *m*-dimensional interest rate structure, with $X_t = Y_t/M_t$ defines the vector of the interest-rate factors that bond prices are linear of. On the other hand, the specification of the innovation dynamics on $(\alpha + \beta Z_t) \in \mathbb{R}^{(m+1)\times 1}$ determines the pricing of interest-rate options. In particular, the innovation Z_t can have an *n*-dimensional stochastic volatility structure to capture the independent variation of interest-rate implied volatilities.

1.2.1. Specification analysis of interest-rate transition dynamics and bond pricing

From equation (25), the fair values of zero-coupon bonds become,

$$P(t,T) = \mathbb{E}_t\left[\frac{M_T}{M_t}\right] = \frac{1}{M_t}\nu^\top e^{-AT}\left(\alpha + \beta Z_t\right) = \nu^\top e^{-A\tau} X_t, \tag{26}$$

where the time-homogeneous coefficients $\nu^\top e^{-A\tau}$ determine the shape of the interest-rate term structure and the loading on the transformed interest-rate factors X_t. While X_t have $(m+1)$ elements, the constraint $M_t = \nu^\top Y_t$ reduces one degree of freedom, resulting in an m-dimensional term structure. In particular, for $P(t,t) = 1$, we need $\nu^\top X_t = 1$.

The bond pricing equation in (26) involves evaluating a matrix exponential $e^{-A\tau}$ at each maturity. The following proposition diagonalizes the matrix to enhance identification and computation.

Proposition 2 *If the transition matrix A has distinct real eigenvalues, one can diagonalize the transition matrix A_d while setting $\nu_d = (1,\cdots,1)^\top$ without losing any generality. Specifically, let D denote the diagonal matrix made of the eigenvalues of A and V denote the matrix made of the eigenvectors, the diagonalized transition matrix is simply $A_d = D$ and the ith element of the transformed interest-rate factors become $\{X_t^d\}_i = \{V^{-1}X_t\}_i/\{V^\top\nu\}_i$. To guarantee $P(t,t) = 1$, we ask $\sum_{i=0}^m \{X_t^d\}_i = 1$ for all t.*

Proof. With V and D being the two matrices made of the eigenvectors and eigenvalues of matrix A, we have $A = VDV^{-1}$ and thus $e^{-A\tau} = Ve^{-D\tau}V^{-1}$. The bond pricing equation becomes,

$$P(t,T) = \nu^\top e^{-A\tau}X_t = \nu^\top Ve^{-D\tau}V^{-1}X_t = \widetilde{\nu}^\top e^{-D\tau}\widetilde{X}_t, \tag{27}$$

with $\widetilde{\nu} = V^\top\nu$ and $\widetilde{X}_t = V^{-1}X_t$. The above transformation converts the transition matrix into a diagonal matrix made of the eigenvalues of the original matrix $A_d = D$. To transform the loading to be a vector of ones, we have

$$P(t,T) = \widetilde{\nu}^\top e^{-D\tau}\widetilde{X}_t = \sum_i \widetilde{\nu}_i e^{-D_{ii}\tau}\widetilde{X}_t^i = \sum_i e^{-D_{ii}\tau}(\widetilde{\nu}_i\widetilde{X}_t^i) = \nu_d^\top e^{-A_d\tau}X_t^d, \tag{28}$$

with $\nu_d = (1,\cdots,1)^\top$, $A_d = D$, and $\{X_t^d\}_i = \{V^{-1}X_t\}_i/\{V^\top\nu\}_i$. ■

We can represent the diagonalized transition matrix as $A = \theta_r I_{m+1} + \langle\kappa_0,\kappa_1,\cdots,\kappa_m\rangle$ with $0 = \kappa_0 < \kappa_1 < ... < \kappa_m$, I_{m+1} being an $(m+1)$-dimensional identity matrix, and $\langle\cdot\rangle$ denoting a diagonal matrix with the diagonal elements given in the brackets. With this representation, we can set $X_t^0 = 1 - \sum_{i=1}^m X_t^i$, so that the bond pricing can be written as

$$P(t,T) = \nu^\top e^{-A\tau}X_t = e^{-\theta_r\tau}\sum_{i=0}^{m+1} e^{-\kappa_j\tau}X_t^i = e^{-\theta_r\tau}\left(1 - \sum_{i=1}^m (1-e^{-\kappa_i\tau})X_t^i\right). \tag{29}$$

In our one-factor example in section 1.1, we can set

$$\nu = \begin{pmatrix} 1 \\ 0 \end{pmatrix}, \quad A = \theta_r I_2 + \begin{pmatrix} 0 & 1 \\ 0 & \kappa \end{pmatrix}, \quad X_t = \begin{pmatrix} 1 \\ x_t \end{pmatrix}, \tag{30}$$

or equivalently we can use the following diagonal representation:

$$\nu = \begin{pmatrix} 1 \\ 1 \end{pmatrix}, \quad A = \theta_r I_2 + \begin{pmatrix} 0 & 0 \\ 0 & \kappa \end{pmatrix}, \quad X_t = \begin{pmatrix} 1 - \frac{x_t}{\kappa} \\ \frac{x_t}{\kappa} \end{pmatrix}. \tag{31}$$

1.2.2. Specification analysis of interest-rate volatility dynamics and option pricing

To price options, we retain the $(\alpha + \beta Z_t)$ innovation specification. With the diagonalized representation of the interest-rate factors, the jth element of Y_t becomes $Y_t^i = e^{-(\theta_r + \kappa_i)t}\{\alpha + \beta Z_t\}_i$, and the time-$T$ price on the bond portfolio becomes,

$$\widehat{P}_T = \frac{1}{M_T} \sum_{i=0}^{m} \left(\sum_{s=1}^{N} c_s e^{-(\theta_r + \kappa_i)s} R(T,s) \right) \{\alpha + \beta Z_T\}_i. \tag{32}$$

Option valuation on this bond portfolio is analogous to the one-factor example.

Proposition 3 *The time-t value V_t of an European option on the bond portfolio that pays off $\Pi_T = (D\widehat{P}_T - K)^+$ is given by*

$$V_t = \mathbb{E}_t \left[\frac{M_T}{M_t} \left(D\widehat{P}_T - K \right)^+ \right] = \mathbb{E}_t \left[(F_t + G_t Z_T)^+ \right] \tag{33}$$

where the deterministic coefficients F_t and G_t are given by

$$F_t = \frac{\nu^\top \left(\sum_s e^{-As} \eta_s R(T,s) \right) \alpha}{\nu^\top e^{-At} (\alpha + \beta Z_t)}, \qquad G_t = \frac{\nu^\top \left(\sum_s e^{-As} \eta_s R(T,s) \right) \beta}{\nu^\top e^{-At} (\alpha + \beta Z_t)} \tag{34}$$

with $\eta_s = Dc_s$ for $s > T$ and $\eta_T = Dc_T - K$.

Proof. The bond portfolio with cash-flows η_s has time T price $\widetilde{P}_T = D\widehat{P}_T - K$. Recall $M_t = \nu^\top e^{-At}(\alpha + \beta Z_t)$, and calculate

$$\begin{aligned} M_t V_t &= \mathbb{E}_t\left[M_T\left(\widetilde{P}_T\right)^+\right] = \mathbb{E}_t\left[\left(\nu^\top\left(\sum_s e^{-As}\eta_s R(T,s)\right)(\alpha+\beta Z_T)\right)^+\right] \\ &= \mathbb{E}_t\left[\left(\widetilde{F}_t + \widetilde{G}_t Z_T\right)^+\right], \end{aligned}$$

with

$$\widetilde{F} = \nu^\top\left(\sum_s e^{-As}\eta_s R(T,s)\right)\alpha, \quad \widetilde{G}_t = \nu^\top\left(\sum_s e^{-As}\eta_s R(T,s)\right)\beta$$

and $F_t = \widetilde{F}_t/M_t$, $G_t = \widetilde{G}_t/M_t$. ■

The pricing of interest-rate options depends on the specification of the Z_t dynamics. For tractability, we let (α,β) be $(m+1)$-dimensional vectors $\{\alpha_i,\beta_i\}_{i=0}^m$ and specify Z_t as an exponential martingale. Then, if Z_t follows a geometric Brownian motion, the Black-Scholes formula in (24) still holds. More generally, to capture the time variation of the interest rate volatility, we propose the following generic model structure for the Z_t dynamics to accommodate multiple sources of stochastic volatility,

$$\begin{aligned} dZ_t/Z_t &= \textstyle\sum_{j=1}^n \sqrt{v_t^j}\, dW_t^j, \\ dv_t^j &= \kappa_{vj}\left(\theta_{vj} - v_t^j\right)dt + \sigma_{vj}\sqrt{v_t^j}\, dW_t^{vj}, \end{aligned} \tag{35}$$

where we model the instantaneous return on Z_t as driven by multiple Brownian motion components, each driven by stochastic volatility. Furthermore, we allow correlation between each Brownian innovation in Z_t and the corresponding Brownian innovation in its stochastic variance rate, $\rho_j dt = \mathbb{E}[dW_t^j dW_t^{vj}]$. All other pairs of Brownian motions are assumed to be independent of each another. This specification can capture the term structure variation through different mean reversion speeds κ_{vj}. For identification, we rank the mean-reversion speeds as $\kappa_1 < \cdots < \kappa_n$. Furthermore, through multiple innovation components on Z_t, the specification also has the potential to generate variations in the implied volatility skew along the strike dimension. We can easily incorporate discontinuous movements in the Z_t dynamics and in the stochastic variance rates while maintaining pricing tractability. One approach to do this is to follow the time-changed Lévy process specification of Carr and Wu (2004). Incorporating jumps has been proven helpful in more accurately capturing the pricing behavior of short-term far out-of-the-money options. Nevertheless, for

model estimation, we only obtain at-the-money swaptions data. Hence, we focus on purely continuous specifications for parsimony.

Under this specification, the log return on Z_t can be written as a linear combination of n time-changed Brownian motions,

$$\ln Z_T/Z_t = \sum_{j=1}^{n} W^j_{\mathcal{T}^j_{t,T}} - \frac{1}{2}\mathcal{T}^j_{t,T}, \tag{36}$$

where the stochastic time changes are defined by the instantaneous variance rates,

$$\mathcal{T}^j_{t,T} \equiv \int_t^T v^j_s ds. \tag{37}$$

With this representation, we can derive its Fourier transform as exponential affine functions of the variance rates,

$$\phi(u) \equiv \mathbb{E}_t\left[e^{iu\ln Z_T/Z_t}\right] = \exp\left(-\sum_{j=1}^{n}\left(a_j(\tau) - b_j(\tau)^\top v^j_t\right)\right), \tag{38}$$

where the time-homogeneous coefficients can be solved analytically,

$$\begin{array}{rcl} b_j(t) & = & \frac{2\psi(u)\left(1-e^{-\xi_j\tau}\right)}{2\xi_j-\left(\xi_j-\kappa^{\mathbb{M}}_{vj}\right)\left(1-e^{-\xi_j\tau}\right)}, \quad \xi_j = \sqrt{\left(\kappa^{\mathbb{M}}_{vj}\right)^2 + 2\sigma^2_{vj}\psi(u)}, \\ a_j(t) & = & \frac{\kappa_{vj}\theta_{vj}}{\sigma^2_{vj}}\left[2\ln\left(1-\frac{\xi_j-\kappa^{\mathbb{M}}_{vj}}{2\xi_j}\left(1-e^{-\xi_j\tau}\right)\right) + (\xi_j-\kappa^{\mathbb{M}}_{vj})\tau\right], \end{array} \tag{39}$$

with $\kappa^{\mathbb{M}}_{vj} = \kappa_{vj} - iu\sigma_{vj}\rho_j$ and $\psi(u) = \frac{1}{2}(iu+u^2)$. Once we have the Fourier transform $\phi(u)$, we can solve the option value defined in (33) numerically through various methods of fast Fourier inversions (Wu (2008)).

The interest-rate factors X_t and the diagonalized transition matrix A can be estimated from the interest rate term structure. To map the identified interest rate factors X_t to the $(\alpha+\beta Z_t)$ representation, we note that

$$X_t = Y_t/M_t = \frac{e^{-At}(\alpha+\beta Z_t)}{\nu^\top e^{-At}(\alpha+\beta Z_t)}.$$

The relation is time-inhomogeneous. In particular, it has the undesirable behavior that as calendar time goes to infinity $t\to\infty$, $X_j \to 0$ for $j = 1,\cdots,m$. To avoid this undesirable behavior, we normalize the calendar time to zero at each time and further normalize $M_0 = 1$ and $Z_0 = 1$. Then, we map the loading coefficients (α,β) to the estimated interest-rate factors X on that date.

In the one-factor case, equation (19) shows that the upper bound of x_t declines with increasing β_0. Setting $\beta_0 = 0$ generates the highest upper bound at κ. We henceforth apply this constraint of $\beta_0 = 0$. To make the lower bound lower than the upper bound, we need $\alpha_0 > 0$. With a strictly positive α_0, the lower bound declines as α_1 decreases. To guarantee positive rates, we set $x_{\min}(0) + \theta_r = 0$, from which we have $\alpha_1 = -\alpha_0 \left(\frac{\theta_r}{\theta_r+\kappa}\right)$. Combining these conditions with the normalization $M_0 = \alpha_0 + \beta_0 + \alpha_1 + \beta_1 = 1$ further pins down $\beta_1 = 1 - \alpha_0 \frac{\kappa}{\theta_r+\kappa}$. To guarantee positivity on β_1, we need $0 < \alpha_0 < \frac{\theta_r+\kappa}{\kappa}$. Thus, we achieve full identification with $X = 1 - \alpha_0$, from which we can represent all loading coefficients (α, β) as a function of X and the model parameters (θ_r, κ). In the multifactor case, we analogously set $\beta_0 = 0$, and

$$\alpha_j = -z_j \frac{\theta_r}{\theta_r + \kappa_j}, \quad \beta_j = 1 - z_j \frac{\kappa_j}{\theta_r + \kappa_j}, \quad j \geq 1. \tag{40}$$

Then, we can solve $z_j = 1 - X_j$ and $\alpha_0 = 1 - \sum_{i=1}^{m} X_i$ to achieve the identification.

1.3. Representing swaptions as options on bond portfolios

Actively traded interest rate derivatives such as caps, floors, and swaptions can all be represented as European options on a portfolio of zero-coupon bonds and can thus all be priced according to Proposition 3. We use swaptions as an example and show how to link the contract details to the cashflow coefficients in Proposition 3.

A plain-vanilla interest-rate swap is an agreement between two parties to exchange a fixed for a floating set of payments at specified future dates. The fixed leg is made of fixed payments of Sh multiplied by a notional amount, where S denotes the fixed rate, and h is the frequency or tenor of the swap contract, represented in fraction of a year. For standard U.S. dollar interest-rate swaps, the tenor is usually half year, $h = 1/2$. The ith fixed payment is paid in arrears at the $(i+1)$th period. The floating leg is also paid in arrears, with the ith payment being $LIBOR(T_i, T_i + h)h$ multiplied by the notional amount, where $LIBOR(T_i, T_i + h)$ denotes the time-T_i LIBOR of maturity h, which is related to the time-T_i zero-coupon bond prices by,

$$LIBOR(T_i, T_i + h) = \frac{1}{h}\left(\frac{1}{\widehat{P}(T_i, T_i + h)} - 1\right). \tag{41}$$

The time-T swap rate is the fixed rate that sets the time-T values of the two legs equal to each other. For a spot-starting ($T_1 = T$) swap contract with N payments with tenor h, the time-T swap rate that sets the contract to zero value is related to the zero-coupon bond prices by,

$$S(T,Nh) = \frac{1-\widehat{P}(T,T+(N+1)h)}{\sum_{i=1}^{N} h\widehat{P}(T,T+(i+1)h)}. \tag{42}$$

A European swaption is a contract that gives the holder the right at time T to enter a swap contract (to pay or receive the fixed rate over the life of the swap) of h tenor and N payments at a pre-known rate K. In this contract, T is the option maturity, K is the option strike. Assuming that the option gives the holder the right to enter a spot-starting swap, we can write the payoff to the payer's swaption as,

$$\Pi_T = (S(T,Nh)-K)^+ \sum_{i=1}^{N} h\widehat{P}(T,T+(i+1)h). \tag{43}$$

Plug the swap rate valuation equation (42) into the payoff function, we have

$$\Pi_T = \left(1-\widehat{P}(T,T+(N+1)h) - K\sum_{i=1}^{N} h\widehat{P}(T,T+(i+1)h)\right)^+. \tag{44}$$

Thus, the payer's swaption can be regarded as a put option with maturity T and strike 1 on a portfolio of zero-coupon bonds, with the coupon schedule given by $c_i = \{Kh+\delta_N\}_{i=1}^N$ paid at $T+(i+1)h$, where δ_N is an indicator function that is one when $i = N$ and zero otherwise. Accordingly, we can obtain the value of the swaption by applying Proposition 3, with $\eta_T = 1$ and $\eta_s = -c_i$ for $s = \{T+(i+1)h\}_{i=1}^N$.

2. Data analysis

We estimate the interest-rate factor transition dynamics using U.S. dollar LIBOR and swap rates and the interest-rate volatility dynamics using U.S. dollar swaptions. We collect a decade worth of over-the-counter quotes on (i) six LIBOR series at fixed time to maturities of one, two, three, six, nine, and 12 months, (ii) nine swap rate series at fixed time to maturities of two, three, four, five, seven, 10, 15, 20, and 30 years, and (iii) 70 at-the-money swaption implied volatility series at a fixed grid of seven swap maturities at one, two,

three, four, five, seven, and 10 years and ten option maturities at one, three, six months and one, two, three, four, five, seven, and 10 years. The data are sampled weekly (every Wednesday) from August 19, 1998 to August 20, 2008, 523 weekly observations for each series.

2.1. Quoting conventions

The U.S. dollar LIBOR rates are simply compounded interest rates, related to the zero-coupon bond prices according to equation (41), where the time to maturity h is computed following actual over 360 day counting convention, starting two business days forward. The U.S. dollar swap rates have payment intervals of half years ($h = 0.5$) and are related to the zero-coupon bond prices according to equation (42).

The swaption contracts are quoted in terms of the Black implied volatility, obtained under the assumption that the underlying forward swap rate is log-normally distributed. Given an implied volatility quote IV, the invoice price for the payer's swaption with one dollar notional is computed as,

$$SWAPTION(t,T,Nh) = (S(t,T,Nh)\mathcal{N}(d_1) - K\mathcal{N}(d_2))\sum_{i=1}^{N} h\widehat{P}(t,T+(i+1)h), \tag{45}$$

where $\mathcal{N}(\cdot)$ denotes the standard cumulative normal function with the two standardized variables (d_1,d_2) given by

$$d_1 = \frac{\ln S(t,T,Nh)/K + \frac{1}{2}IV^2(T-t)}{IV\sqrt{T-t}}, \quad d_2 = d_1 - IV\sqrt{T-t}, \tag{46}$$

and $S(t,T,Nh)$ denotes the time-t forward starting swap rate that starts at time T with N payments and a payment interval of h. The forward starting swap rate is related to the zero-coupon bond prices by

$$S(t,T,Nh) = \frac{\widehat{P}(t,T) - \widehat{P}(t,T+(N+1)h)}{\sum_{i=1}^{N} h\widehat{P}(t,T+(i+1)h)}. \tag{47}$$

The at-the-money swaptions have the strikes set to the corresponding forward starting swap rate, in which case we can rewrite the Black formula in (45) as

$$ATMSN(t,T,Nh) = \left(\widehat{P}(t,T) - \widehat{P}(t,T+(N+1)h)\right)(2\mathcal{N}(d)-1), \tag{48}$$

with $d = \frac{1}{2}IV\sqrt{T-t}$.

2.2. Summary statistics

Table 1 reports the summary statistics on the LIBOR and swap rates. The average interest rates exhibit an upward sloping term structure. The standard deviation estimates of the interest rates largely decrease with increasing maturity, but the standard deviation estimates on the weekly changes of the interest rates are in similar ranges across all maturities, with no clear term structure pattern. The interest rates are all highly persistent, more so at short term than at long term. The skewness and excess kurtosis estimates are small for the interest rate levels, but the kurtosis estimates are large for weekly changes on the short-term LIBOR series, reflecting the effect of the discrete Federal Reserve policy moves.

The left panel of Figure 1 plots the time series of the three-month LIBOR (solid line), and the two-year (dashed line) and 30-year (dash-dotted line) swap rates. During our sample period, the three-month LIBOR has moved over a wide range from as low as 1% (in June 2003) to as high as 6.86% (in May 2000). The 30-year swap rate does not vary as much, thus generating term structure variations as the LIBOR moves. The right panel plots some representative term structures of the interest rates at different rates, including an upward sloping (dashed line on August 13, 2003), a downward sloping (dash-dotted line on September 12, 2007) and a relatively flat (dotted line on October 11, 2006) term structure. The upward-sloping solid line represents the mean term structure.

[Figure 1 about here.]

Table 2 reports the summary statistics of the swaption implied volatility quotes. Each panel represents one summary statistic. Within each panel, each column represents one option maturity and each row represents one underlying swap maturity. Panel A reports the sample averages of implied volatility series. On average, the implied volatility is higher at short option maturities and shorter-term swaps. The average implied volatility decline along the underlying swap maturity reflects the mean-reversion behavior of interest-rate factors, which results in long-term rates being less volatile than short-term rates. On the other hand, the volatility decline along the option maturity reflects the mean reversion behavior of the interest-rate volatility factors. Panels B and C report the standard deviation estimates of the implied volatility levels and weekly changes, respectively. In both panels, the standard deviation estimates decline with both increasing option maturities and swap maturities. Panel D reports the weekly autocorrelation estimates on the implied

volatility series. The estimates are largely comparable across swap maturities, but show some declining pattern along the option maturities. Figure 2 visualizes the summary statistics of the implied volatility series along the two maturity dimensions. One interesting feature from Tables 1 and 2 is that both interest rates and interest-rate options show more persistence at short maturities than at long maturities.

[Figure 2 about here.]

Figure 3 plots the implied volatility time series at selected interest-rate and option maturities. The two panels represent two different swap maturities, with the first panel showing options on one-year swap and the second panel showing options on ten-year swap. The three lines in each panel represent three different option maturities at one year (solid lines), five years (dashed lines), and ten years (dashed dotted lines). Implied volatilities at the same option maturities show similar time series behaviors across different underlying interest-rate maturities. Comparing the interest rate time series in Figure 1 with the implied volatility time series in Figure 3, we find that the implied volatilities are high during the low interest-rate eras.

[Figure 3 about here.]

To understand the driving forces behind the interest-rate implied volatility variations, we perform principal component analysis on the implied volatility series. Figure 4 plots in the first panel the ten largest normalized eigenvalues of the correlation matrix of the weekly changes on 70 the implied volatility series, which can be interpreted as the percentage variation explained by each principal component. The first principal component explains 78% of the variation, the second explains 12%, and the third explains 4%. The remaining principal components all together explain less than 7% of the variation. The remaining three panels in Figure 4 plot the loading of the first three principal components on the 70 implied volatility series along the seven swap maturity and ten option maturity dimensions. The first component is relatively flat across all swap and option maturities, representing the variation on the interest-rate volatility level. The second principal component loading positively at short option maturities but negatively at long option maturities, generating a term structure variation along the option maturity dimension. The third principal component forms a tented shape along the option maturity dimension, representing a curvature factor on

option maturities. The loadings of all three principal components are relatively flat along the swap maturity dimension.

[Figure 4 about here.]

3. Model estimation

Our modeling framework provides a separation of the interest-rate factors and the interest-rate volatility factors. The former governs the interest-rate term structure variation whereas the latter governs the variation of the option implied volatilities term structure for a given underlying interest rate series. Accordingly, our model estimation also takes a two-step procedure. In the first step, we estimate the transition matrix A and extract the interest-rate factors X_t to fit the LIBOR and swap rates term structure. In the second step, we take the estimated transition matrix as given and estimate the loading coefficients (α, β), the volatility dynamics, and extract the volatility factors to match the implied volatility surface of caps and swaptions. At each step, we cast the model into a state-space form and estimate the dynamics using a quasi-maximum likelihood method.

In the first step, we take the interest-rate factor X_t as the hidden state vector and the LIBOR/swap rates as our observations. We estimate both a one-factor and a three-factor specification, both taking the diagonalized representation in (31) and (29), respectively. We approximate the state propagation equation using a simple AR(1) specification,

$$X_t = A + \Phi X_{t-1} + \sqrt{Q}\varepsilon_t, \tag{49}$$

where we let Φ be a diagonal matrix and assume that the standardized innovation ε_t is normally distributed. Under the risk-neutral measure, the diagonalized factors have zero mean and time-varying mean-reversion speeds $(\kappa_j - x_t)$ that are declining with increasing short rate level. In the state-propagation equation (49), we allow non-zero means and assume constant mean-reversion speeds for all factors under the statistical measure. These assumptions can be regarded either as driven by risk premium assumptions or simply

approximations of the actual statistical dynamics that we leave unspecified. To construct the measurement equations, we assume that the LIBOR and swap rates are observed with additive, normally distributed errors,

$$\begin{pmatrix} LIBOR(t,t+m/12) \\ SWAP(t,2\tau) \end{pmatrix} = f(X_t;\Theta) + \sqrt{R}e_t, \qquad \begin{array}{l} m = 1,2,3,6,9,12 \text{ months}, \\ \tau = 2,3,4,5,7,10,15,20,30 \text{ years}, \end{array} \tag{50}$$

where $f(X_t;\Theta)$ denotes the corresponding LIBOR/swap value generated from the model at the state level X_t and the parameter set Θ. We assume that the measurement errors from different series are identical and independent of one another with a constant pricing error variance σ_r^2.

In the second step, we take the variance risk factors V_t as the hidden state vector and the swaptions as the observations. We estimate models with one, two, and three stochastic variance factors, respectively, conditional on both one and three interest-rate factors from the first stage. In each case, we specify the state-propagation equation as a discrete-time analog of its statistical dynamics, and we construct the measurement equations by adding additive, normally distributed errors to the at-the-money swaption prices,

$$ATMSN(t,\tau_o,\tau_s) = f^o(X_t;\Theta_o) + \sqrt{R}e_t^o, \qquad \begin{array}{l} \tau_O = \frac{1}{12},\frac{3}{12},\frac{6}{12},1,2,3,4,5,7,10, \\ \tau_S = 1,2,3,4,5,7,10, \end{array} \tag{51}$$

where τ_O, τ_S denote the time to maturities (in years) of swaptions, and the underlying swaps. We first convert the implied volatility quotes into invoice prices, and then scale the invoice price by the Black vega of each contract. With this scaling, we assume that the measurement errors are iid with variance constant at σ_o^2.

When both the state propagation equation and the measurement equations are Gaussian and linear, the Kalman (1960) filter generates efficient forecasts and updates on the conditional mean and covariance of the state vector and the measurement series. In our application, the measurement equations in (50) and (51) are nonlinear. We use the unscented Kalman filter (Wan and van der Merwe (2001)) to handle the nonlinearity. The unscented Kalman filter approximates the posterior state density using a set of deterministically chosen sample points (sigma points). These sample points completely capture the mean and covariance of the Gaussian state variables, and when propagated through the nonlinear functions in the measurement equations, capture the posterior mean and covariance of the measurement series accurately to the second order for any nonlinearity. Appendix B provides the technical details for the filtering methodology.

Given the predicted mean and covariance matrix on the measurement series, we construct the log-likelihood value assuming normally distributed forecasting errors. We maximize the sum of log-likelihood value to estimate the model parameters. We keep the long-run mean of the short rate (θ_r) fixed from the first-stage estimation, but we re-estimate the interest-rate transition coefficient κ in the second stage to achieve a better fitting of the implied volatility behavior along the swap maturity dimension.

4. Term structure of interest rates

Table 3 reports the summary statistics of the pricing errors from the one-factor and three-factor term structure models. The pricing errors are defined as the difference in basis points between the observed LIBOR and swap rates and the model-implied values. As expected, the three-factor model performs much better than the one-factor model. On average, the one-factor model explains 84.1% of the variation in the interest rate series, but the three-factor model explains over 98.6%. The estimated one-factor model explains the short-term interest-rate variation reasonably well, but fails miserably in pricing long-term swap rates. By contrast, the three-factor model explains all series by over 96%: The mean pricing errors are all within four basis points. The root mean squared pricing errors are between five to 35 basis points, larger for long-term LIBOR and short-term swap rates, but smaller for short-term LIBOR and long-term swap rates. The larger errors between three month to two year maturities are in part driven by the discrepancies between LIBOR and swap rates (Babbs and Webber (1995)).

Table 4 reports the first-stage estimates and the absolute magnitude of the *t*-statistics (in parentheses) on the interest-rate factor dynamics. The one-factor specification generates a mean-reversion speed of 0.2110. For the three-factor model, the long-run mean of the short rate is estimated at 5.85% and the three mean-reversion speeds that underly the transition matrix are estimated at 0.0242, 0.3650, and 1.3745, respectively, allowing the three factors to capture interest-rate movements of different frequencies.

Figure 5 shows how shocks on the three interest-rate factors impact the interest-rate term structure differently. The solid lines in each panel plot the continuously compounded spot rates as a function of maturity, generated by the three-factor model with factors set to their sample averages. The dashed lines denote the yield curve generated by setting one of the three factors to its 90th percentile value and while

setting the other two to their respective sample averages. The dash-dotted lines are generated by setting one of the three factors to its 10th percentile value while setting the other two to their respective sample averages. The first panel shows that moving the first interest-rate factor from its mean value to its 90th and 10th percentiles generates parallel shifts on the yield curve. Thus, shocks on the first factor incur relatively uniform responses from the yield curve across all maturities. By contrast, the second panel shows that shocks on the second factor generate larger movements at the short term than at the long term of the yield curve, consistent with the lower risk-neutral persistence of the second factor. The third factor is even less persistent, and accordingly, shocks on the third factor show up mainly at the very short end of the yield curve maturities, as shown in the third panel. The response declines rapidly as the interest-rate maturity increases.

[Figure 5 about here.]

To gain intuition on the diagonalized interest-rate factors X_t, we can perform the following transformation,

$$\begin{aligned} c_t &= \kappa_c(\kappa_c-\kappa_x)(\kappa_c-\kappa_s)X_t^1, \\ s_t &= -\kappa_c(\kappa_c-\kappa_x)X_t^1-\kappa_s(\kappa_s-\kappa_x)X_t^2, \\ x_t &= \kappa_c X_t^1+\kappa_s X_t^2+\kappa_x X_t^3. \end{aligned} \tag{52}$$

The transformed factor x_t is simply the short-rate gap with $r_t = x_t + \theta_r$ and is related to the other two factors through the following risk-neutral transition dynamics,

$$\begin{aligned} \mathbb{E}_t^{\mathbb{Q}}[dx_t] &= (s_t-(\kappa_x-x_t)x_t)\,dt, \\ \mathbb{E}_t^{\mathbb{Q}}[ds_t] &= (c_t-(\kappa_s-x_t)s_t)\,dt, \\ \mathbb{E}_t^{\mathbb{Q}}[dc_t] &= -(\kappa_c-x_t)\,c_t dt. \end{aligned} \tag{53}$$

The short rate gap x_t mean-reverts to a stochastic level s_t, which mean-reverts to yet another stochastic level c_t, which is centered around zero. The sequence of reversion dictates that shocks on x_t mainly impact the short-term of the interest-rate term structure while shocks on c_t, or equivalently the first element of X_t, generate persistent impacts on the yield curve across the whole term structure. The effects of s_t are somewhere in the middle. For all three factors, the mean-reversion speeds, ($\kappa_x - x_t$, $\kappa_s - x_t$, and $\kappa_c - x_t$) are not constant, but are all stochastic and decline with increasing interest-rate levels.

Figure 6 plots the time series of the three interest-rate factors, both in the diagonalized form X_t (on the left side) and in the transformed short rate space (x_t, s_t, c_t) (on the right side). The extracted $x_t + \theta_r$ matches the short-term LIBOR well.

[Figure 6 about here.]

5. Interest rate volatility term structures

In the second stage, we estimate six models with the $(m+n)$ factor structure, with $m = 1, 3$ and $n = 1, 2, 3$. Table 5 reports the mean pricing error on the swaption implied volatilities from the six models. Pricing errors are defined as the difference between the implied volatility quotes and the model-generated values, in percentage points. All six models show similar mean pricing bias patterns along the two maturity dimensions (option maturity τ_O and swap maturity τ_S). The mean pricing errors are negative for short-term options on short-term swaps, and also slightly negative for long-term options on long-term swaps. On the other hand, the mean pricing errors are positive for short-term options on long-term swaps and long-term options on short-term swaps. The mean pricing errors are particularly large on short-term options on the one-year swap. This large negative mean error is potentially related to the large negative mean pricing error on the 12-month LIBOR. Due to institutional details, the yield curve often show distortions in linking six-month and 12-month LIBOR to the swap rates. Our model does not have an explicit adjustment for this distortion, and it also shows up in the pricing of short-term options on the one-year swap. The mean pricing errors on other swap and option maturities are much smaller, mostly within two volatility points for all six models.

Table 6 reports the root mean squared pricing errors from the six models. Increasing the number of interest-rate factors and the number of volatility factors both help reduce the root mean square pricing error estimates. For the $(3+3)$ model, the root mean squared pricing errors are only one volatility point or less for moderate maturity options on moderate maturity swaps. Table 7 reports the explained variation on each series from each of the six models. Overall, the explained variation is higher at short option maturities than at long option maturities. The $(3+3)$ model explains most moderate-maturity options over 90%.

Table 8 reports the second-stage estimates and absolute values of the *t*-statistics (in parentheses) on the model parameters that govern the stochastic volatility dynamics. Given the large amount of swaption quotes (36,610) used for estimating the models, all parameters are estimated with strong statistical significance. When we re-estimate the interest-rate transition dynamics (κ) to match the implied volatility surface behavior along the swap maturity dimension, the estimates for the first two factors are both much smaller than those estimated from the interest rates. The high persistence is needed to generate the high implied volatility observed from swaptions at long swap maturities. The estimates for the mean-reversion speed (κ_v) of the first volatility factor are also very small. The high volatility persistence is needed to generate the observed high implied volatility at long option maturities. When we estimate the $(3+3)$ model, the last element for κ and the last element for κ_v are both very large, suggesting that a highly transient interest-rate and volatility component is needed to specifically capture the behavior of short-term options on short-term swaps.

In Figure 7, we take the $(3+3)$ model and generate implied volatility term structures across the option maturity dimension (left side) and the swap maturity dimension (right panel). The solid lines in each panel are generated from the model with all interest-rate and volatility factors set to their sample average. The dashed lines and the dash-dotted lines are generated by changing one of the volatility factors to its 90th and 10th percentile value, respectively.

[Figure 7 about here.]

From the three panels on the left side, we observe distinct responses from the swaption implied volatilities along the option maturity dimension to shocks on the three volatility factors. When we shock the first volatility factor v_t^1 (top left panel), the implied volatilities response across all option maturities. The persistent response is in line with the low mean reversion speed estimate on this volatility factor. On the other hand, when we shock the second volatility factor, the responses are large at short option maturities but dissipate quickly as the option maturity increases. The speed of dissipation is even faster for the more transient third volatility factor.

The three panels on the right side show a completely different picture about the implied volatility responses along the swap maturity dimension. The variations are largely constant as the underlying swap

maturity varies, suggesting that the volatility dynamics mainly generate variations along the option maturity dimension, not the swap maturity dimension.

Figure 8 plots the time series of the three interest-rate volatility factors extracted from the $(3+3)$ model. The first factor is the most persistent factor. Its variation matches the variation of swaption implied volatilities at long option maturities. On the other hand, the other two factors capture more transient variations of swaption implied volatilities at short option maturities. In particular, the most recent spike in swaption implied volatility is mostly attributed to spikes in the more transient second and third volatility factors.

[Figure 8 about here.]

6. Concluding remarks

Traditional models often link the interest-rate volatility to the curvature of the yield curve; yet evidence shows that a large proportion of the variation in interest-rate option implied volatilities is independent of the variation of the yield curve. The linearity-generating framework proposed by Gabaix (2007) provides a natural reconciliation between theory and the evidence. Under this framework, bond prices are linear in a set of yield curve factors. As a result, only the risk-neutral drift, or the transition dynamics, of the interest-rate factors enter the bond pricing equation, but neither volatilities of these factors nor the volatility dynamics affect bond pricing. Therefore, if these factors show stochastic volatility, these stochastic volatilities are truly unspanned and completely un-identified from the yield curve.

In this paper, we perform specification analysis on the linearity-generating framework, and analyze how one can identify the interest-rate factor transition dynamics from the yield curve and how one can identify the interest-rate volatility dynamics from interest-rate options. We show within this framework how one can tractably price options through a Fourier transform approach on any bond portfolios with multi-dimensional stochastic volatility structures. We also propose a sequential identification procedure under which we estimate the interest-rate transition dynamics from LIBOR and swap rates, and then estimate the volatility dynamics from interest-rate options. Through model design and estimation, we show how the

interest-rate factor transition dynamics and the volatility structures affect the swaption implied volatility differently across the option maturity and the underlying swap maturity.

The specification analysis in this paper paves the ground for many potential applications and extensions. For example, when one needs to price options across a wide range of strikes, one can readily extend the innovation specification to allow discontinuous movements in interest rates and/or interest-rate volatilities. One can also use the same dynamic specification to price both caps and swaptions, and explore the potential discrepancies between the two options markets. From a broader perspective, our analysis also provides a road map to address long-standing economic questions by exploiting information in both the interest-rate term structure and the interest-rate option implied volatilities. The options data are likely to provide information regarding the level and dynamics of uncertainty about monetary policy, as well as the degree of credibility of the central bank's commitment to its inflation target.

Appendix A. Derivation details on the one-factor example

The one-factor example can be represented as,

$$Y_t = \begin{pmatrix} 1-\frac{x_t}{\kappa} \\ \frac{x_t}{\kappa} \end{pmatrix} M_t, \tag{A1}$$

where M_t denotes the state price deflator.

A.1. The transition matrix

Under the specification in (A1), we can show that the $\mathbb{P}$-dynamics of Y_t is controlled by the transition matrix $A = \begin{pmatrix} \theta_r & 0 \\ 0 & \kappa+\theta_r \end{pmatrix}$ as in equation (9).

Proof.

$$\begin{aligned}
\mathbb{E}_t\left[dY_t^{(1)}\right] &= \mathbb{E}_t\left[d\left(1-\frac{x_t}{\kappa}\right)M_t\right] \\
&= \left(1-\frac{x_t}{\kappa}\right)M_t\mathbb{E}_t\left[\frac{dM_t}{M_t}\right] - \frac{M_t}{\kappa}\mathbb{E}_t\left[dx_t\right] - \frac{M_t}{\kappa}\left\langle dx_t, \frac{dM}{M_t}\right\rangle \\
&= -\left(1-\frac{x_t}{\kappa}\right)M_t r_t dt - \frac{M_t}{\kappa}\left(\mathbb{E}_t\left[dx_t\right] + \left\langle dx_t, \frac{dM}{M_t}\right\rangle\right) \\
&= -\left(1-\frac{x_t}{\kappa}\right)M_t r_t dt - \frac{M_t}{\kappa}\mathbb{E}_t^{\mathbb{Q}}\left[dx_t\right] \\
&= -\left(1-\frac{x_t}{\kappa}\right)M_t\left(x_t+\theta_r\right)dt + \frac{M_t}{\kappa}x_t\left(\kappa-x_t\right)dt \\
&= \left(1-\frac{x_t}{\kappa}\right)M_t\left[-\left(x_t+\theta_r\right)+x_t\right]dt \\
&= -\theta_r Y_t^{(1)}dt.
\end{aligned}$$

$$\begin{aligned}
\mathbb{E}_t\left[dY_t^{(2)}\right] &= \mathbb{E}_t\left[d\frac{x_t}{\kappa}M_t\right] \\
&= \frac{x_t}{\kappa}M_t\mathbb{E}_t\left[\frac{dM_t}{M_t}\right] + \frac{M_t}{\kappa}\mathbb{E}_t\left[dx_t\right] + \frac{M_t}{\kappa}\left\langle dx_t, \frac{dM}{M_t}\right\rangle \\
&= -\frac{x_t}{\kappa}M_t r_t dt + \frac{M_t}{\kappa}\left(\mathbb{E}_t\left[dx_t\right] + \left\langle dx_t, \frac{dM}{M_t}\right\rangle\right) \\
&= -\frac{x_t}{\kappa}M_t r_t dt - \frac{M_t}{\kappa}x_t\left(\kappa-x_t\right)dt \\
&= \left(-x_t-\theta_r-\kappa+x_t\right)\frac{x_t}{\kappa}M_t \\
&= -\left(\theta_r+\kappa\right)Y_t^{(1)}dt.
\end{aligned}$$

■

A.2. The short rate dynamics and risk premium

To derive the short rate dynamics and the risk premium in terms of the Z_t representation, we note that

$$\begin{aligned} M_t &= e^{-\theta_r t}\left((\alpha_0+\beta_0 Z_t)+e^{-\kappa t}(\alpha_1+\beta_1 Z_t)\right), \\ r_t &= \theta_r + x_t, \\ x_t &= \frac{\kappa e^{-\kappa t}(\alpha_1+\beta_1 Z_t)}{((\alpha_0+\beta_0 Z_t)+e^{-\kappa t}(\alpha_1+\beta_1 Z_t))} = \frac{1}{M_t}\kappa e^{-(\theta_r+\kappa)t}(\alpha_1+\beta_1 Z_t). \end{aligned}$$

First, we derive the dynamics for the state price deflator M_t,

$$\begin{aligned} \frac{dM_t}{M_t} &= \frac{\left(-\theta_r e^{-\theta_r t}(\alpha_0+\beta_0 Z_t)-(\theta_r+\kappa)e^{-(\theta_r+\kappa)t}(\alpha_1+\beta_1 Z_t)\right)}{M_t}dt \\ &\quad + \frac{(\beta_0+e^{-\kappa t}\beta_1)}{(\alpha_0+\beta_0 Z_t)+e^{-\kappa t}(\alpha_1+\beta_1 Z_t)}dZ_t, \end{aligned}$$

where the negative of the diffusion coefficient

$$\gamma(Z) = -\frac{(\beta_0+e^{-\kappa t}\beta_1)}{(\alpha_0+\beta_0 Z_t)+e^{-\kappa t}(\alpha_1+\beta_1 Z_t)}$$

defines the market price of the Z risk. The drift component of the state price deflator is the negative of the short rate,

$$\begin{aligned} \frac{\mathbb{E}_t[dM_t]/dt}{M_t} &= \frac{-\theta_r e^{-\theta_r t}(\alpha_0+\beta_0 Z_t)-(\theta_r+\kappa)e^{-(\theta_r+\kappa)t}(\alpha_1+\beta_1 Z_t)}{M_t} \\ &= \frac{-\theta_r M_t - \kappa e^{-(\theta_r+\kappa)t}(\alpha_1+\beta_1 Z_t)}{M_t} \\ &= -\theta_r - x_t = -r_t. \end{aligned}$$

To derive the dynamics for x_t, we note that

$$\frac{dM_t x_t}{M_t} = x_t\frac{dM_t}{M_t} + dx_t + \left\langle dx_t, \frac{dM_t}{M_t}\right\rangle.$$

Thus, the risk-neutral drift of x_t is given by

$$\begin{aligned}\mathbb{E}_t^{\mathbb{Q}}[dx_t] &= \mathbb{E}_t[dx_t] + \left\langle dx_t, \frac{dM_t}{M_t} \right\rangle \\ &= \frac{d\mathbb{E}_t[M_t x_t]}{M_t} - x_t \frac{d\mathbb{E}_t[M_t]}{M_t}.\end{aligned}$$

As $M_t x_t = \kappa e^{-(\theta_r+\kappa)t}(\alpha_1 + \beta_1 Z_t)$, we have

$$\frac{d\mathbb{E}_t[M_t x_t]}{M_t} = -(\theta_r + \kappa) x_t dt.$$

Thus,

$$\begin{aligned}\mathbb{E}_t^{\mathbb{Q}}[dx_t] &= -(\theta_r+\kappa) x_t dt + x_t(\theta_r + x_t) dt \\ &= -x_t(\kappa - x_t) dt,\end{aligned}$$

which is the same as the specification in (6).

The martingale component of x_t is given by $x_Z dZ$, with

$$\begin{aligned}x_Z &= \frac{\kappa e^{-\kappa t}\beta_1}{(\alpha_0+\beta_0 Z_t) + e^{-\kappa t}(\alpha_1+\beta_1 Z_t)} - \frac{\kappa e^{-\kappa t}(\alpha_1+\beta_1 Z_t)(\beta_0 + e^{-\kappa t}\beta_1)}{((\alpha_0+\beta_0 Z_t) + e^{-\kappa t}(\alpha_1+\beta_1 Z_t))^2} \\ &= \frac{\kappa e^{-\kappa t}(\alpha_0\beta_1 - \alpha_1\beta_0)}{((\alpha_0+\beta_0 Z_t) + e^{-\kappa t}(\alpha_1+\beta_1 Z_t))^2} \\ &= \frac{(x_{\max}-x)(x-x_{\min})}{x_{\max}-x_{\min}} \frac{1}{Z_t},\end{aligned}$$

with

$$x_{\min} = \frac{\kappa e^{-\kappa t}\alpha_1}{\alpha_0 + e^{-\kappa t}\alpha_1},\ x_{\max} = \frac{\kappa e^{-\kappa t}\beta_1}{\beta_0 + e^{-\kappa t}\beta_1}.$$

The instantaneous risk premium of the short rate is given by the negative of the covariance term $\left\langle dx_t, \frac{dM_t}{M_t} \right\rangle$,

$$\begin{aligned}\left\langle dx_t, \frac{dM_t}{M_t} \right\rangle &= \left\langle x_Z dZ_t, \frac{M_Z}{M_t} dZ_t \right\rangle = x_Z \frac{M_z}{M_t} \langle dZ_t \rangle \\ &= \frac{(x_{\max}-x)(x-x_{\min})}{x_{\max}-x_{\min}} \frac{e^{-\theta_r t}(\beta_0 + e^{-\kappa t}\beta_1)}{M_t} \frac{\langle dZ_t \rangle}{Z_t}.\end{aligned}$$

Since the covariance is positive, the instantaneous risk premium on the interest rate is negative.

Appendix B. Unscented Kalman filter and maximum likelihood estimation

To estimate the model parameters, we cast the model into a state-space form, which consists of a set of state propagation equations and measurement equations. We rewrite them in canonical forms,

$$x_t = A + \Phi x_{t-1} + \sqrt{Q_{t-1}}\varepsilon_t, \quad \varepsilon_t \sim N(0, I), \tag{B2}$$

$$y_t = h(x_t) + e_t, \quad e_t \sim N(0, R). \tag{B3}$$

Let $\overline{x}_t, \overline{V}_t, \overline{y}_t, \overline{A}_t$ denote the time-$(t-1)$ ex ante forecasts of time-t values of the state vector, the covariance of the state vector, the measurement series, and the covariance of the measurement series. Let $\widehat{x}_t$ and $\widehat{V}_t$ denote the ex post update, or filtering, on the state vector and its covariance at the time t based on observations (y_t) at time t. In the case of linear measurement equations,

$$y_t = Hx_t + e_t, \tag{B4}$$

the Kalman filter provides the most efficient updates. The ex ante predictions are,

$$\begin{array}{lllll} \overline{x}_t &=& A + \Phi\widehat{x}_{t-1}, & \overline{V}_t &= \Phi\widehat{V}_{t-1}\Phi^\top + Q_{t-1}; \\ \overline{y}_t &=& H\overline{x}_t, & \overline{A}_t &= H\overline{V}_t H^\top + R, \end{array} \tag{B5}$$

and the ex post filtering updates are,

$$\widehat{x}_{t+1} = \overline{x}_{t+1} + K_{t+1}\left(y_{t+1} - \overline{y}_{t+1}\right), \quad \widehat{V}_{t+1} = \overline{V}_{t+1} - K_{t+1}\overline{A}_{t+1}K_{t+1}^\top, \tag{B6}$$

where K_{t+1} is the Kalman gain, given by $K_{t+1} = \overline{V}_{t+1}H^\top\left(H\overline{V}_{t+1}H^\top + R\right)^{-1}$. In essence, the Kalman filter generates the state updates as a weighted average between the forecasted values $\overline{x}_{t+1}$ and the new observations y_{t+1}, with the weight determined by the relative magnitudes of the state forecasting error variance ($\overline{V}_{t+1}$) and the observation measurement error variance (R).

In our application, the measurement equation in (B3) is nonlinear. Hence, we cannot directly apply the Kalman filter procedure described in (B5) and (B6). Traditionally, the nonlinearity is often handled by the Extended Kalman Filter (EKF), which approximates the nonlinear measurement equation with a linear expansion, evaluated at the predicted states:

$$y_t \approx H_t x_t + e_t, \quad H_t = \left.\frac{\partial h(x_t)}{\partial x_t}\right|_{x_t = \overline{x}_t}. \tag{B7}$$

By contrast, the unscented Kalman filter applied in this paper uses a set of deterministically chosen (sigma) points to directly approximate the distribution of the state vector. The predictions and updates are directly performed on these

sigma points, with the mean and covariance of the states and measurements computed from these points. Specifically, let p be the number of states and $\delta > 0$ be a control parameter. A set of $2p+1$ sigma vectors χ_i are generated according to the following equations:

$$\begin{aligned} \chi_{t,0} &= \widehat{x}_t, \\ \chi_{t,i} &= \widehat{x}_t \pm \sqrt{(p+\delta)(\widehat{V}_t+Q)_j}, \quad j=1,\cdots,p; \quad i=1,\cdots,2p, \end{aligned} \tag{B8}$$

with corresponding weights w_i given by

$$w_0 = \delta/(p+\delta), \quad w_i = 1/[2(p+\delta)], \quad j=1,\cdots,2p. \tag{B9}$$

We can regard these sigma vectors as forming a discrete distribution with w_i being the corresponding probabilities. We can verify that the mean, covariance, skewness, and kurtosis of this distribution are $\widehat{X}_t$, $\widehat{V}_t+Q$, 0, and $p+\delta$ respectively.

Given the sigma points, the prediction steps are given by

$$\begin{aligned} \overline{\chi}_{t,i} &= A+\Phi\chi_{t,i}, & \overline{\xi}_{t,i} &= h(\overline{\chi}_{t,i}) \\ \overline{x}_{t+1} &= \textstyle\sum_{i=0}^{2p} w_i\overline{\chi}_{t,i}, & \overline{V}_{t+1} &= \textstyle\sum_{i=0}^{2p} w_i(\overline{\chi}_{t,i}-\overline{x}_{t+1})(\overline{\chi}_{t,i}-\overline{x}_{t+1})^\top; \\ \overline{y}_{t+1} &= \textstyle\sum_{i=0}^{2p} w_i\overline{\xi}_{t,i}, & \overline{A}_{t+1} &= \textstyle\sum_{i=0}^{2p} w_i\left[\overline{\xi}_{t,i}-\overline{y}_{t+1}\right]\left[\overline{\xi}_{t,i}-\overline{y}_{t+1}\right]^\top + R, \end{aligned} \tag{B10}$$

and the filtering updates are

$$\widehat{x}_{t+1} = \overline{x}_{t+1} + K_{t+1}\left(y_{t+1}-\overline{y}_{t+1}\right), \quad \widehat{V}_{t+1} = \overline{V}_{t+1} - K_{t+1}\overline{A}_{t+1}K_{t+1}^\top, \tag{B11}$$

with the Kalman gain given by

$$K_{t+1} = S_{t+1}\left(\overline{A}_{t+1}\right)^{-1}, \quad S_{t+1} = \sum_{i=0}^{2p} w_i\left[\overline{\chi}_{t,i}-\overline{x}_{t+1}\right]\left[\overline{\xi}_{t,i}-\overline{y}_{t+1}\right]^\top. \tag{B12}$$

To estimate the model parameters Θ, we define the log likelihood for each day's observation assuming that the forecasting errors are normally distributed:

$$l_t(\Theta) = -\frac{1}{2}\log\left|\overline{A}_t\right| - \frac{1}{2}\left(\left(y_t-\overline{y}_t\right)^\top\left(\overline{A}_t\right)^{-1}\left(y_t-\overline{y}_t\right)\right). \tag{B13}$$

We maximize the sum of the log likelihood values to obtain the model parameters,

$$\Theta \equiv \arg\max_{\Theta} \sum_{t=1}^{N} l_t(\Theta), \tag{B14}$$

where N denotes number of weeks in our sample.

References

Babbs, S. H., and N. J. Webber, 1995, "Term Structure Modeling under Alternative Official Regimes," FORC preprint 95/61, University of Warwick.

Carr, P., and L. Wu, 2004, "Time-Changed Lévy Processes and Option Pricing," *Journal of Financial Economics*, 71(1), 113–141.

Carr, P., and L. Wu, 2006, "A Tale of Two Indices," *Journal of Derivatives*, 13(3), 13–39.

Cochrane, J., 2004, *Asset Pricing*. Princeton University Press, Princeton, NJ.

Collin-Dufresne, P., and R. S. Goldstein, 2002, "Do Bonds Span the Fixed Income Markets? Theory and Evidence for Unspanned Stochastic Volatility," *Journal of Finance*, 57(4), 1685–1730.

Cox, J. C., J. E. Ingersoll, and S. R. Ross, 1985, "A Theory of the Term Structure of Interest Rates," *Econometrica*, 53(2), 385–408.

Dai, Q., and K. Singleton, 2003, "Term Structure Dynamics in Theory and Reality," *Review of Financial Studies*, 16(3), 631–678.

Duffie, D., 1992, *Dynamic Asset Pricing Theory*. Princeton University Press, Princeton, New Jersey, second edn.

Duffie, D., J. Pan, and K. Singleton, 2000, "Transform Analysis and Asset Pricing for Affine Jump Diffusions," *Econometrica*, 68(6), 1343–1376.

Gabaix, X., 2007, "Linearity-Generating Processes: A Modelling Tool Yielding Closed Forms for Asset Prices," working paper, New York University.

Harrison, M., and D. Kreps, 1979, "Martingales and Arbitrage in Multiperiod Security Markets," *Journal of Economic Theory*, 20, 381–408.

Heath, D., R. Jarrow, and A. Morton, 1992, "Bond Pricing and the Term Structure of Interest Rates: A New Technology for Contingent Claims Valuation," *Econometrica*, 60(1), 77–105.

Heidari, M., A. Hirsa, and D. B. Madan, 2007, "Pricing of Swaptions in Affine Term Structures with Stochastic Volatility," in *Advances in Mathematical Finance*, ed. by M. C. Fu, R. A. Jarrow, J.-Y. J. Yen, and R. J. Elliott. Birkhäuser Boston, pp. 173–193.

Heidari, M., and L. Wu, 2003, "Are Interest Rate Derivatives Spanned by the Term Structure of Interest Rates?," *Journal of Fixed Income*, 13(1), 75–86.

Heidari, M., and L. Wu, 2008, "Term Structure of Interest Rates, Yield Curve Residuals, and the Consistent Pricing of Interest-Rate Derivatives," *Journal of Financial and Quantitative Analysis*, forthcoming.

Hull, J., and A. White, 1990, "Pricing Interest-Rate Derivative Securities," *Review of Financial Studies*, 3(4), 573–592.

Jacod, J., and A. N. Shiryaev, 1987, *Limit Theorems for Stochastic Processes*. Springer-Verlag, Berlin.

Kalman, R. E., 1960, "A New Approach to Linear Filtering and Prediction Problems," *Transactions of the ASME–Journal of Basic Engineering*, 82(Series D), 35–45.

Leippold, M., and L. Wu, 2003, "Design and Estimation of Quadratic Term Structure Models," *European Finance Review*, 7(1), 47–73.

Li, H., and F. Zhao, 2006, "Unspanned Stochastic Volatility: Evidence from Hedging Interest Rate Derivatives," *Journal of Finance*, 61(1), 341–378.

Rogers, L., and D. Williams, 1987, *Diffusions, Markov Processes, and Martingales*, vol. 2. John Wiley & Sons, New York.

Schrager, D., and A. Pelsser, 2006, "Pricing Swaptions and Coupon Bond Options in Affine Term Structure Models," *Mathematical Finance*, 16(4), 673–694.

Vasicek, O. A., 1977, "An Equilibrium Characterization of the Term Structure," *Journal of Financial Economics*, 5(2), 177–188.

Wan, E. A., and R. van der Merwe, 2001, "The Unscented Kalman Filter," in *Kalman Filtering and Neural Networks*, ed. by S. Haykin. Wiley & Sons Publishing, New York.

Wu, L., 2008, "Modeling Financial Security Returns Using Lévy Processes," in *Handbook of Financial Engineering*, ed. by J. Birge, and V. Linetsky. Elsevier, New York.

Table 1
Summary statistics of LIBOR and swap rates

Maturity	Levels					Weekly differences		
	Mean	Std	Skew	Kurt	Auto	Std	Skew	Kurt
1m	3.752	1.828	-0.093	-1.457	0.997	0.108	-1.314	24.580
2m	3.789	1.831	-0.105	-1.450	0.997	0.090	-1.765	24.256
3m	3.825	1.838	-0.105	-1.433	0.998	0.086	-2.461	19.642
6m	3.897	1.824	-0.112	-1.364	0.998	0.091	-2.311	11.841
9m	3.961	1.802	-0.094	-1.284	0.997	0.102	-1.484	6.874
12m	4.040	1.773	-0.070	-1.195	0.997	0.114	-0.901	3.999
2y	4.308	1.555	0.042	-0.884	0.995	0.135	0.002	0.560
3y	4.561	1.380	0.148	-0.671	0.993	0.142	0.078	0.450
4y	4.757	1.251	0.260	-0.529	0.992	0.143	0.117	0.417
5y	4.917	1.155	0.372	-0.435	0.991	0.144	0.099	0.476
7y	5.154	1.024	0.552	-0.307	0.989	0.140	0.137	0.381
10y	5.386	0.915	0.716	-0.209	0.988	0.135	0.141	0.354
15y	5.623	0.820	0.806	-0.203	0.987	0.127	0.140	0.244
20y	5.726	0.774	0.793	-0.258	0.986	0.122	0.087	0.227
30y	5.763	0.745	0.789	-0.267	0.986	0.117	0.086	0.261

Entries report the summary statistics of the six LIBOR series and nine swap rate series, including sample mean, standard deviation (Std), skewness (Skew), excess kurtosis (Kurt), and weekly autocorrelation (Auto). Data are weekly (on Wednesdays) from August 19, 1998 to August 20, 2008, 523 observations for each series.

Table 2
Summary statistics of swaption implied volatilities

Rate\Option	$\frac{1}{12}$	$\frac{3}{12}$	$\frac{6}{12}$	1	2	3	4	5	7	10
A. Mean										
1	26.60	26.65	27.57	26.98	23.89	21.80	20.33	19.28	17.37	15.11
2	28.41	28.03	27.11	25.34	22.67	20.92	19.65	18.65	16.83	14.60
3	26.48	26.10	25.31	23.79	21.68	20.24	19.08	18.18	16.39	14.22
4	25.05	24.80	24.09	22.72	20.93	19.66	18.60	17.72	15.99	13.86
5	24.13	23.89	23.22	21.94	20.33	19.16	18.16	17.29	15.57	13.49
7	21.98	21.89	21.46	20.55	19.32	18.32	17.41	16.60	14.99	13.04
10	19.99	20.00	19.77	19.13	18.19	17.35	16.53	15.76	14.31	12.48
B. Standard deviation										
1	16.33	15.54	15.44	13.06	8.19	5.55	4.01	3.14	2.27	1.70
2	16.25	15.31	13.69	10.74	6.99	4.93	3.72	2.97	2.24	1.73
3	13.58	12.67	11.28	8.99	6.06	4.46	3.43	2.78	2.17	1.74
4	11.78	11.06	9.81	7.86	5.44	4.08	3.21	2.63	2.09	1.75
5	10.68	10.00	8.88	7.13	5.01	3.80	3.03	2.50	2.05	1.79
7	8.44	7.93	7.08	5.83	4.30	3.33	2.71	2.26	1.92	1.77
10	6.61	6.17	5.57	4.67	3.56	2.81	2.33	1.99	1.81	1.73
C. Standard deviation on weekly changes										
1	3.50	2.86	2.46	1.95	1.29	1.00	0.86	0.73	0.58	0.52
2	3.07	2.50	1.99	1.61	1.14	0.95	0.77	0.71	0.57	0.52
3	2.53	2.07	1.74	1.44	1.01	0.86	0.71	0.63	0.55	0.48
4	2.32	1.77	1.48	1.19	0.94	0.78	0.69	0.61	0.54	0.46
5	2.18	1.66	1.34	1.10	0.87	0.75	0.67	0.60	0.53	0.47
7	1.86	1.38	1.15	0.92	0.77	0.68	0.62	0.57	0.48	0.44
10	1.66	1.18	0.98	0.79	0.69	0.63	0.58	0.53	0.49	0.47
D. Weekly autocorrelation										
1	0.976	0.982	0.986	0.987	0.986	0.981	0.974	0.970	0.964	0.951
2	0.980	0.985	0.988	0.987	0.985	0.979	0.975	0.968	0.964	0.953
3	0.981	0.985	0.986	0.985	0.984	0.978	0.975	0.970	0.965	0.960
4	0.979	0.985	0.986	0.986	0.983	0.979	0.973	0.969	0.964	0.963
5	0.977	0.984	0.986	0.985	0.983	0.977	0.972	0.968	0.963	0.963
7	0.973	0.982	0.984	0.985	0.981	0.976	0.970	0.964	0.965	0.966
10	0.966	0.979	0.982	0.983	0.978	0.971	0.964	0.960	0.959	0.960

Entries report the summary statistics of the swaption implied volatilities. Each panel represents one summary statistic. Within each panel, each column represents one option maturity and each row represents one underlying swap maturity. Data are weekly (on Wednesdays) from August 19, 1998 to August 20, 2008, 523 observations for each series.

Table 3
Summary statistics of the pricing errors on LIBOR/swap rates

	One-factor model							Three-factor model						
Maturity	Mean	Rmse	Skew	Kurt	Max	Auto	VR	Mean	Rmse	Skew	Kurt	Max	Auto	VR
1 m	0.861	38.715	-0.271	-0.469	110.454	0.972	95.506	-1.307	8.530	-1.248	1.678	34.316	0.898	99.787
2 m	1.066	36.204	-0.274	-0.466	99.764	0.981	96.086	0.154	14.527	-0.913	1.022	53.193	0.913	99.369
3 m	1.221	33.977	-0.260	-0.466	94.651	0.984	96.580	1.389	20.553	-0.743	1.137	71.878	0.939	98.753
6 m	-1.909	29.381	-0.297	-0.746	74.328	0.982	97.411	0.590	29.777	-1.043	0.832	110.659	0.949	97.330
9 m	-5.576	26.359	-0.166	-0.863	69.824	0.972	97.953	-1.814	33.201	-1.198	1.180	131.062	0.945	96.610
12 m	-7.487	24.676	0.002	-0.765	68.640	0.954	98.237	-3.234	34.203	-1.256	1.408	140.015	0.938	96.303
2 y	-1.600	25.897	-0.433	-0.091	83.428	0.929	97.230	0.623	23.521	-1.392	1.835	100.415	0.965	97.708
3 y	2.115	32.651	-0.021	0.280	99.368	0.944	94.417	0.931	16.219	-1.328	1.609	63.080	0.952	98.621
4 y	3.651	37.856	0.236	0.059	113.203	0.954	90.906	-0.251	12.492	-1.096	1.204	48.854	0.939	99.001
5 y	4.380	41.627	0.320	-0.256	122.392	0.960	87.122	-1.205	10.588	-0.986	0.949	41.431	0.939	99.169
7 y	4.001	46.063	0.304	-0.699	124.207	0.967	79.877	-2.502	9.066	-0.795	0.664	34.323	0.939	99.274
10 y	2.408	49.507	0.212	-1.022	117.933	0.971	70.743	-2.353	8.071	-0.857	0.429	28.758	0.935	99.287
15 y	1.997	52.532	0.088	-1.194	110.526	0.976	58.959	1.704	6.032	-1.375	1.393	20.991	0.938	99.501
20 y	-0.854	53.242	0.025	-1.234	101.226	0.977	52.609	2.341	5.932	-1.481	2.587	21.209	0.920	99.503
30 y	-9.640	54.126	0.070	-1.178	108.739	0.978	48.735	-2.577	6.577	-1.174	2.239	30.775	0.909	99.338
Average	-0.358	38.854	-0.031	-0.607	99.912	0.967	84.158	-0.501	15.953	-1.126	1.344	62.064	0.935	98.637

Entries report the summary statistics of the pricing errors on the LIBOR and swap rates, defined as the basis-point difference between the observed LIBOR/swap rates and the model-implied values for both the one-factor model and the three-factor model. The statistics include the sample averages of the pricing error (Mean), the root mean squared pricing error (Rmse), skewness (Skew), excess kurtosis (Kurt), maximum absolute error (Max), weekly autocorrelation (Auto), and the percentage explained variation (VR), defined as one minus the ratio of pricing error variance to the variance of the original interest-rate series.

Table 4
First-stage estimates on interest-rate factor dynamics

Θ_r	θ_r	κ	A	Φ	Q	σ_r^2
1-factor	$\begin{bmatrix} 0.0643 \\ (962.7) \end{bmatrix}$	$\begin{bmatrix} 0.2110 \\ (170.0) \end{bmatrix}$	$\begin{bmatrix} 0.0000 \\ (-) \end{bmatrix}$	$\begin{bmatrix} 1.0000 \\ (-) \end{bmatrix}$	$\begin{bmatrix} 2.5e-5 \\ (10.0) \end{bmatrix}$	$\begin{bmatrix} 0.1638 \\ (148.5) \end{bmatrix}$
3-factor	$\begin{bmatrix} 0.0585 \\ (188.9) \end{bmatrix}$	$\begin{bmatrix} 0.0242 \\ (24.2) \\ 0.3650 \\ (110.6) \\ 1.3745 \\ (76.6) \end{bmatrix}$	$\begin{bmatrix} -0.0006 \\ (0.2) \\ 0.0000 \\ (0.0) \\ 0.0343 \\ (10.1) \end{bmatrix}$	$\begin{bmatrix} 0.9914 \\ (116.7) \\ 0.9943 \\ (168.4) \\ 0.0007 \\ (0.2) \end{bmatrix}$	$\begin{bmatrix} 0.0040 \\ (10.0) \\ 0.0001 \\ (11.8) \\ 6602.2 \\ (0.1) \end{bmatrix}$	$\begin{bmatrix} 0.0017 \\ (186.3) \end{bmatrix}$

Entries report the first-stage parameter estimates and absolute values of the *t*-statistics (in parentheses) on the one-factor and three-factor interest-rate dynamics. The estimation is based on weekly sampled LIBOR and swap rate data from August 19, 1998 to August 20, 2008, 523 weekly observations for each series.

Table 5
Mean pricing errors on swaption implied volatilities

$(m+n)$	τ_S/τ_O	$\frac{1}{12}$	$\frac{3}{12}$	$\frac{6}{12}$	1	2	3	4	5	7	10
1+1	1	-7.805	-5.586	-2.392	-0.526	0.147	-0.045	0.071	0.616	1.181	1.447
	2	-0.080	0.500	0.745	0.603	0.120	-0.155	0.025	0.140	0.772	1.051
	3	1.436	1.490	1.289	0.712	0.039	-0.146	-0.234	0.093	0.471	0.778
	4	2.088	2.034	1.620	0.812	0.068	-0.318	-0.273	-0.085	0.379	0.527
	5	2.590	2.431	1.909	0.963	-0.031	-0.333	-0.395	-0.304	0.178	0.256
	7	2.258	2.124	1.656	0.806	-0.108	-0.537	-0.566	-0.422	-0.054	-0.027
	10	1.891	1.775	1.402	0.631	-0.221	-0.603	-0.732	-0.683	-0.371	-0.345
1+2	1	-7.667	-6.111	-3.374	-1.538	-0.118	0.278	0.678	1.227	1.194	0.688
	2	-0.088	0.038	-0.071	-0.243	-0.083	0.195	0.642	0.766	0.803	0.315
	3	1.384	1.084	0.582	-0.032	-0.116	0.223	0.397	0.728	0.519	0.063
	4	2.026	1.673	0.989	0.142	-0.049	0.068	0.366	0.560	0.445	-0.167
	5	2.532	2.107	1.337	0.352	-0.119	0.069	0.254	0.351	0.259	-0.419
	7	2.222	1.859	1.168	0.279	-0.145	-0.107	0.101	0.248	0.056	-0.667
	10	1.894	1.578	1.004	0.197	-0.198	-0.139	-0.043	0.009	-0.225	-0.938
1+3	1	-7.741	-6.013	-3.123	-1.280	-0.116	0.093	0.407	0.936	1.003	0.797
	2	-0.159	0.136	0.172	0.007	-0.074	0.020	0.383	0.482	0.616	0.425
	3	1.318	1.183	0.819	0.212	-0.102	0.058	0.145	0.452	0.337	0.175
	4	1.964	1.772	1.220	0.382	-0.031	-0.090	0.123	0.291	0.268	-0.055
	5	2.473	2.206	1.564	0.589	-0.097	-0.082	0.018	0.088	0.087	-0.306
	7	2.171	1.959	1.390	0.511	-0.117	-0.248	-0.123	-0.002	-0.108	-0.553
	10	1.850	1.679	1.221	0.424	-0.164	-0.266	-0.252	-0.226	-0.380	-0.821
3+1	1	-6.665	-5.674	-2.672	-0.918	-0.017	0.061	0.357	0.981	1.446	1.192
	2	0.357	0.363	0.472	0.261	-0.026	-0.051	0.300	0.483	1.018	0.785
	3	1.622	1.328	1.020	0.390	-0.101	-0.048	0.023	0.419	0.700	0.502
	4	2.154	1.853	1.348	0.498	-0.071	-0.235	-0.031	0.223	0.594	0.240
	5	2.586	2.234	1.632	0.652	-0.178	-0.260	-0.169	-0.014	0.380	-0.040
	7	2.173	1.899	1.363	0.487	-0.270	-0.491	-0.370	-0.161	0.121	-0.342
	10	1.737	1.516	1.085	0.293	-0.408	-0.590	-0.577	-0.464	-0.232	-0.683
3+2	1	-6.540	-5.979	-3.231	-1.422	-0.129	0.157	0.505	1.089	1.361	0.962
	2	0.408	0.097	0.010	-0.165	-0.113	0.059	0.457	0.607	0.949	0.570
	3	1.662	1.102	0.622	0.016	-0.165	0.074	0.194	0.555	0.645	0.300
	4	2.199	1.660	0.997	0.163	-0.117	-0.099	0.150	0.372	0.554	0.052
	5	2.641	2.069	1.318	0.348	-0.206	-0.113	0.024	0.147	0.353	-0.216
	7	2.252	1.778	1.104	0.232	-0.267	-0.320	-0.156	0.021	0.119	-0.494
	10	1.850	1.446	0.887	0.097	-0.365	-0.389	-0.334	-0.253	-0.203	-0.805
3+3	1	-6.820	-5.831	-3.030	-1.370	-0.171	0.151	0.539	1.131	1.302	0.937
	2	-0.085	0.212	0.199	-0.121	-0.159	0.048	0.486	0.644	0.887	0.542
	3	1.152	1.205	0.796	0.051	-0.215	0.059	0.218	0.588	0.580	0.269
	4	1.705	1.755	1.158	0.191	-0.169	-0.118	0.169	0.400	0.486	0.019
	5	2.166	2.158	1.468	0.371	-0.262	-0.136	0.038	0.171	0.283	-0.252
	7	1.807	1.857	1.237	0.245	-0.329	-0.350	-0.149	0.037	0.044	-0.536
	10	1.433	1.513	1.001	0.097	-0.435	-0.428	-0.338	-0.247	-0.284	-0.854

Entries report the sample averages of the pricing errors on swaption implied volatilities, defined as the difference in percentage points between the market implied volatility quotes and model-implied values. Each panel represents one model. Within each panel, each column represents one option maturity and each row represents one underlying swap maturity.

Table 6
Root mean squared pricing errors on swaption implied volatilities

$(m+n)$	τ_S/τ_O	$\frac{1}{12}$	$\frac{3}{12}$	$\frac{6}{12}$	1	2	3	4	5	7	10
1+1	1	12.792	8.854	3.932	2.528	2.362	2.135	2.012	2.088	2.098	2.055
	2	2.759	1.811	1.908	2.262	2.122	1.942	1.837	1.759	1.758	1.697
	3	2.900	2.451	2.307	2.276	1.973	1.862	1.729	1.665	1.543	1.477
	4	3.426	3.062	2.714	2.348	1.938	1.765	1.667	1.565	1.441	1.310
	5	3.999	3.622	3.142	2.521	1.901	1.726	1.630	1.499	1.349	1.216
	7	3.368	3.099	2.703	2.264	1.805	1.678	1.586	1.449	1.231	1.113
	10	2.926	2.673	2.425	2.073	1.749	1.646	1.579	1.475	1.234	1.129
1+2	1	11.551	9.141	5.121	2.681	1.350	1.175	1.242	1.618	1.570	1.471
	2	2.037	1.598	1.382	1.163	1.191	1.026	1.132	1.156	1.210	1.233
	3	2.848	2.154	1.601	1.241	1.072	0.994	0.922	1.087	0.985	1.131
	4	3.507	2.816	2.038	1.359	1.086	0.879	0.888	0.937	0.910	1.101
	5	4.100	3.407	2.536	1.612	1.068	0.881	0.813	0.790	0.842	1.171
	7	3.578	3.000	2.202	1.426	1.009	0.818	0.739	0.733	0.762	1.231
	10	3.311	2.705	2.033	1.308	0.960	0.813	0.743	0.711	0.820	1.385
1+3	1	11.499	9.113	5.018	2.530	1.266	1.112	1.145	1.466	1.477	1.440
	2	1.947	1.624	1.358	1.050	1.102	0.973	1.024	1.041	1.134	1.170
	3	2.798	2.180	1.640	1.174	0.995	0.937	0.863	0.974	0.933	1.042
	4	3.476	2.850	2.096	1.332	1.020	0.859	0.836	0.852	0.865	0.990
	5	4.085	3.448	2.601	1.615	1.017	0.864	0.793	0.753	0.825	1.044
	7	3.559	3.034	2.264	1.432	0.968	0.840	0.763	0.720	0.776	1.097
	10	3.290	2.727	2.086	1.313	0.930	0.841	0.793	0.760	0.871	1.246
3+1	1	10.778	8.868	4.511	2.984	1.988	1.886	1.911	2.056	2.183	1.883
	2	2.951	1.755	1.766	1.901	1.717	1.692	1.672	1.756	1.825	1.583
	3	3.393	2.328	2.032	1.838	1.629	1.606	1.613	1.644	1.623	1.417
	4	3.781	2.910	2.406	1.907	1.585	1.575	1.550	1.555	1.503	1.326
	5	4.238	3.450	2.823	2.078	1.596	1.537	1.524	1.491	1.406	1.322
	7	3.469	2.927	2.415	1.890	1.567	1.576	1.523	1.448	1.315	1.317
	10	2.946	2.519	2.190	1.805	1.618	1.616	1.572	1.520	1.339	1.465
3+2	1	10.009	9.050	5.032	2.713	1.158	0.961	1.077	1.435	1.678	1.480
	2	2.393	1.733	1.541	1.242	0.979	0.786	0.882	1.042	1.302	1.207
	3	3.205	2.200	1.717	1.288	0.892	0.748	0.770	0.951	1.099	1.078
	4	3.706	2.805	2.113	1.388	0.911	0.709	0.735	0.847	1.001	1.044
	5	4.213	3.361	2.569	1.619	0.929	0.718	0.705	0.783	0.929	1.102
	7	3.550	2.929	2.218	1.434	0.893	0.767	0.727	0.759	0.873	1.166
	10	3.181	2.618	2.043	1.340	0.914	0.830	0.842	0.882	0.958	1.366
3+3	1	9.917	8.992	4.904	2.524	1.083	0.924	1.092	1.488	1.667	1.436
	2	2.064	1.772	1.383	0.950	0.912	0.748	0.891	1.084	1.294	1.163
	3	2.730	2.221	1.680	1.085	0.822	0.706	0.765	0.985	1.096	1.043
	4	3.219	2.795	2.074	1.193	0.838	0.671	0.724	0.871	0.994	1.014
	5	3.719	3.343	2.544	1.452	0.852	0.678	0.688	0.794	0.928	1.086
	7	3.210	2.916	2.164	1.242	0.827	0.748	0.715	0.768	0.885	1.167
	10	3.071	2.618	1.951	1.120	0.858	0.827	0.840	0.888	0.992	1.382

Entries report the root mean squared pricing errors on swaption implied volatilities, defined as the difference in percentage points between the market implied volatility quotes and model-implied values. Each panel represents one model. Within each panel, each column represents one option maturity and each row represents one underlying swap maturity.

Table 7
Explained variation on swaption implied volatilities

$(m+n)$	τ_S/τ_O	$\frac{1}{12}$	$\frac{3}{12}$	$\frac{6}{12}$	1	2	3	4	5	7	10
1+1	1	0.614	0.804	0.959	0.964	0.917	0.852	0.748	0.597	0.413	0.260
	2	0.971	0.987	0.984	0.959	0.908	0.846	0.756	0.650	0.504	0.407
	3	0.965	0.976	0.971	0.942	0.894	0.826	0.751	0.642	0.540	0.477
	4	0.947	0.957	0.951	0.921	0.873	0.819	0.737	0.645	0.559	0.529
	5	0.919	0.928	0.921	0.893	0.856	0.801	0.727	0.654	0.574	0.560
	7	0.912	0.919	0.909	0.868	0.824	0.772	0.700	0.623	0.591	0.605
	10	0.885	0.895	0.873	0.821	0.762	0.703	0.639	0.569	0.575	0.611
1+2	1	0.720	0.808	0.938	0.972	0.973	0.958	0.932	0.887	0.797	0.413
	2	0.984	0.989	0.990	0.989	0.971	0.958	0.937	0.915	0.837	0.525
	3	0.966	0.978	0.982	0.981	0.969	0.953	0.941	0.915	0.851	0.577
	4	0.941	0.958	0.967	0.970	0.960	0.954	0.936	0.918	0.856	0.612
	5	0.909	0.928	0.941	0.951	0.955	0.947	0.935	0.920	0.847	0.628
	7	0.889	0.912	0.930	0.942	0.946	0.941	0.927	0.907	0.844	0.659
	10	0.831	0.873	0.899	0.923	0.930	0.919	0.899	0.872	0.809	0.651
1+3	1	0.728	0.806	0.935	0.972	0.976	0.960	0.929	0.871	0.771	0.501
	2	0.986	0.989	0.990	0.990	0.975	0.961	0.935	0.903	0.820	0.603
	3	0.967	0.979	0.984	0.983	0.973	0.956	0.938	0.903	0.839	0.650
	4	0.941	0.959	0.970	0.974	0.965	0.956	0.934	0.907	0.845	0.680
	5	0.907	0.930	0.945	0.955	0.959	0.949	0.931	0.910	0.840	0.690
	7	0.888	0.914	0.936	0.947	0.950	0.942	0.922	0.898	0.840	0.714
	10	0.830	0.879	0.907	0.929	0.934	0.919	0.896	0.867	0.811	0.704
3+1	1	0.730	0.807	0.945	0.953	0.941	0.884	0.780	0.669	0.478	0.262
	2	0.967	0.987	0.985	0.969	0.939	0.882	0.804	0.675	0.544	0.369
	3	0.952	0.977	0.976	0.960	0.928	0.870	0.779	0.673	0.543	0.417
	4	0.930	0.959	0.959	0.945	0.915	0.854	0.767	0.656	0.565	0.443
	5	0.901	0.931	0.933	0.923	0.900	0.841	0.750	0.643	0.563	0.457
	7	0.897	0.921	0.921	0.902	0.871	0.798	0.702	0.593	0.536	0.483
	10	0.870	0.894	0.883	0.854	0.807	0.714	0.606	0.471	0.466	0.435
3+2	1	0.784	0.809	0.938	0.969	0.980	0.971	0.944	0.911	0.812	0.560
	2	0.979	0.987	0.987	0.987	0.981	0.975	0.959	0.918	0.842	0.622
	3	0.959	0.977	0.980	0.979	0.979	0.972	0.953	0.923	0.831	0.644
	4	0.936	0.958	0.964	0.969	0.972	0.970	0.950	0.916	0.841	0.644
	5	0.905	0.930	0.938	0.951	0.967	0.965	0.946	0.905	0.824	0.637
	7	0.894	0.914	0.926	0.941	0.961	0.956	0.931	0.887	0.798	0.644
	10	0.846	0.875	0.890	0.918	0.945	0.932	0.890	0.820	0.731	0.591
3+3	1	0.805	0.806	0.938	0.974	0.983	0.973	0.944	0.905	0.789	0.589
	2	0.984	0.987	0.990	0.992	0.983	0.977	0.960	0.914	0.824	0.646
	3	0.967	0.978	0.983	0.985	0.983	0.975	0.954	0.919	0.815	0.663
	4	0.946	0.961	0.969	0.977	0.977	0.974	0.952	0.913	0.828	0.663
	5	0.920	0.935	0.945	0.961	0.974	0.969	0.948	0.903	0.814	0.653
	7	0.901	0.919	0.937	0.956	0.969	0.961	0.933	0.884	0.789	0.657
	10	0.831	0.880	0.909	0.943	0.957	0.937	0.891	0.816	0.723	0.603

Entries report the explained variation on swaption implied volatilities, defined as one minus the ratio of pricing error variance over the variance of the original implied volatility series. Each panel represents one model. Within each panel, each column represents one option maturity and each row represents one underlying swap maturity.

Table 8
Second-stage estimates on interest-rate volatility dynamics

$m+n$	κ	θ_v	κ_v	σ_v	ρ	σ_o^2
1+1	0.0139 (531.6)	5.6874 (213.6)	0.0870 (219.1)	0.4965 (147.8)	−0.1140 (59.3)	0.0008 (839.3)
1+2	0.0158 (687.3)	1.4207 (548.6) 0.9915 (533.3)	0.0000 (0.0) 1.3128 (526.7)	0.2644 (470.1) 2.4900 (579.6)	0.7466 (1733.1) −0.1616 (184.5)	0.0006 (1411.5)
1+3	0.0161 (797.6)	7.2077 (379.6) 0.3659 (455.3) 0.7046 (526.6)	0.0000 (0.0) 1.0089 (812.8) 1.5876 (627.2)	0.2729 (485.6) 1.0045 (494.9) 2.2115 (625.8)	0.6142 (1060) 0.7784 (1950) −0.9977 (2418)	0.0006 (1284)
3+1	0.0000 (238.7) 0.0130 (917.1) 26.2771 (413.2)	2.4293 (386.6)	0.3273 (263.6)	0.7524 (307.1)	−0.2525 (181.5)	0.0007 (918.1)
3+2	0.0003 (790.6) 0.0149 (1178.2) 23.6698 (758.0)	12.6553 (4610.7) 1.1614 (868.9)	0.0001 (813.6) 0.7608 (858.9)	0.3096 (848.5) 1.0858 (1174.2)	0.4318 (723.0) −0.9614 (29045)	0.0006 (1376.6)
3+3	0.0003 (624.2) 0.0145 (940.2) 18.5505 (589.2)	0.0104 (635.6) 0.9965 (658.4) 0.0160 (545.4)	0.0000 (0.0) 1.1875 (571.4) 10.4820 (668.7)	0.3667 (559.7) 2.1048 (762.6) 2.7376 (600.5)	0.3678 (504.1) −0.2784 (512.5) −0.9999 (1205)	0.0005 (1209.8)

Entries report the second-stage parameter estimates and standard errors (in parentheses) on the interest-rate volatility dynamics. The estimation is based on weekly sampled swaptions data from August 19, 1998 to August 20, 2008, 523 weekly observations for each series.

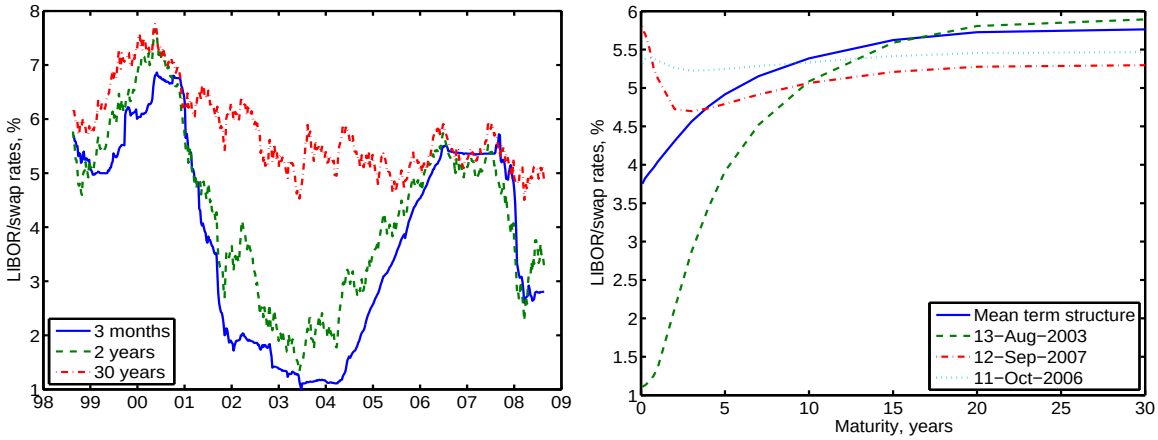

Figure 1

LIBOR/swap rates time series and term structure.

The left panel plots the time series of the three-month LIBOR (solid line), and swap rate at two- (dashed line) and 30-year (dash-dotted line) maturities. The right panel plots the representative term structures at different dates, with the solid line being the mean term structure.

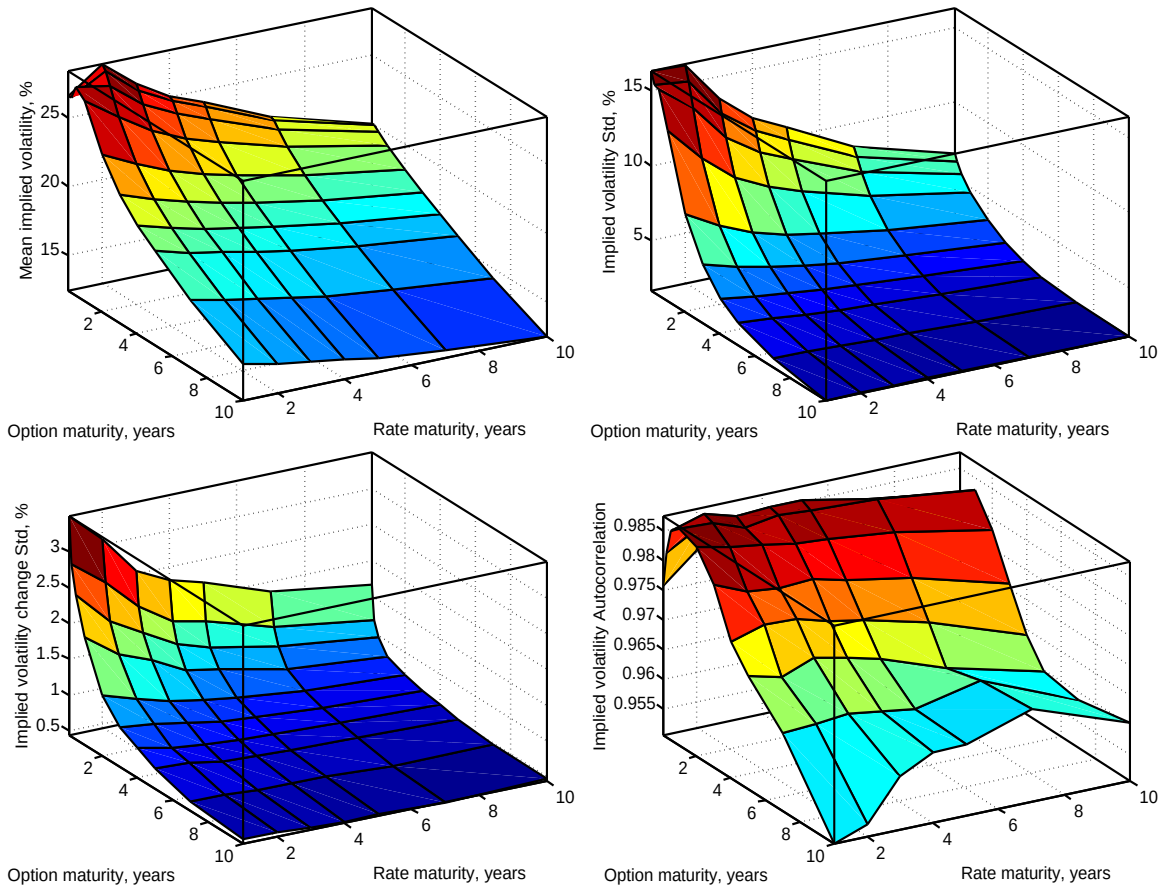

Figure 2

Summary statistics of swaption implied volatilities.

The four panels visualize, respectively, the sample average, the standard deviation, the standard deviation of weekly changes, and the weekly autocorrelation of the swaption implied volatility series across different option and interest-rate maturities.

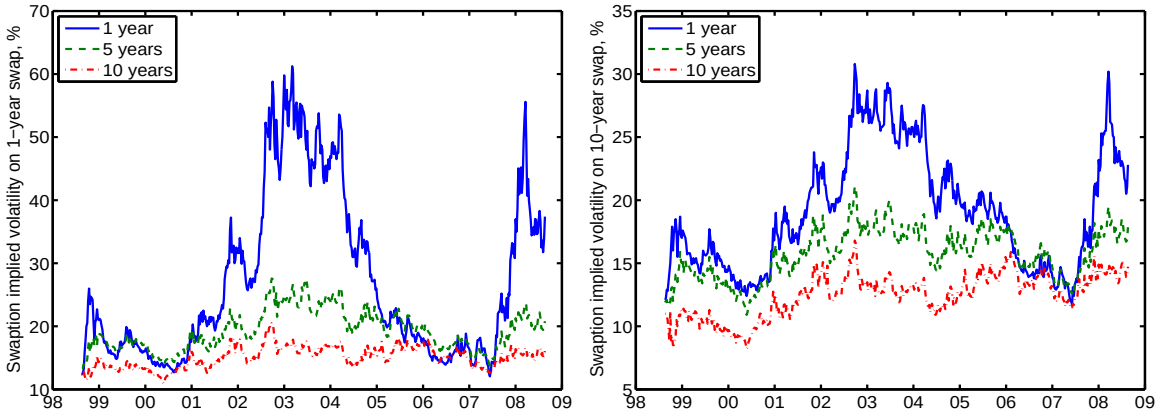

Figure 3

Swaption implied volatility time series.

The two panels are for two different underlying swap maturities at one year (left) and ten years (right), respectively. Within each panel, the three lines denote three option maturities at one year (solid lines), five years (dashed lines), and 10 years (dash-dotted lines).

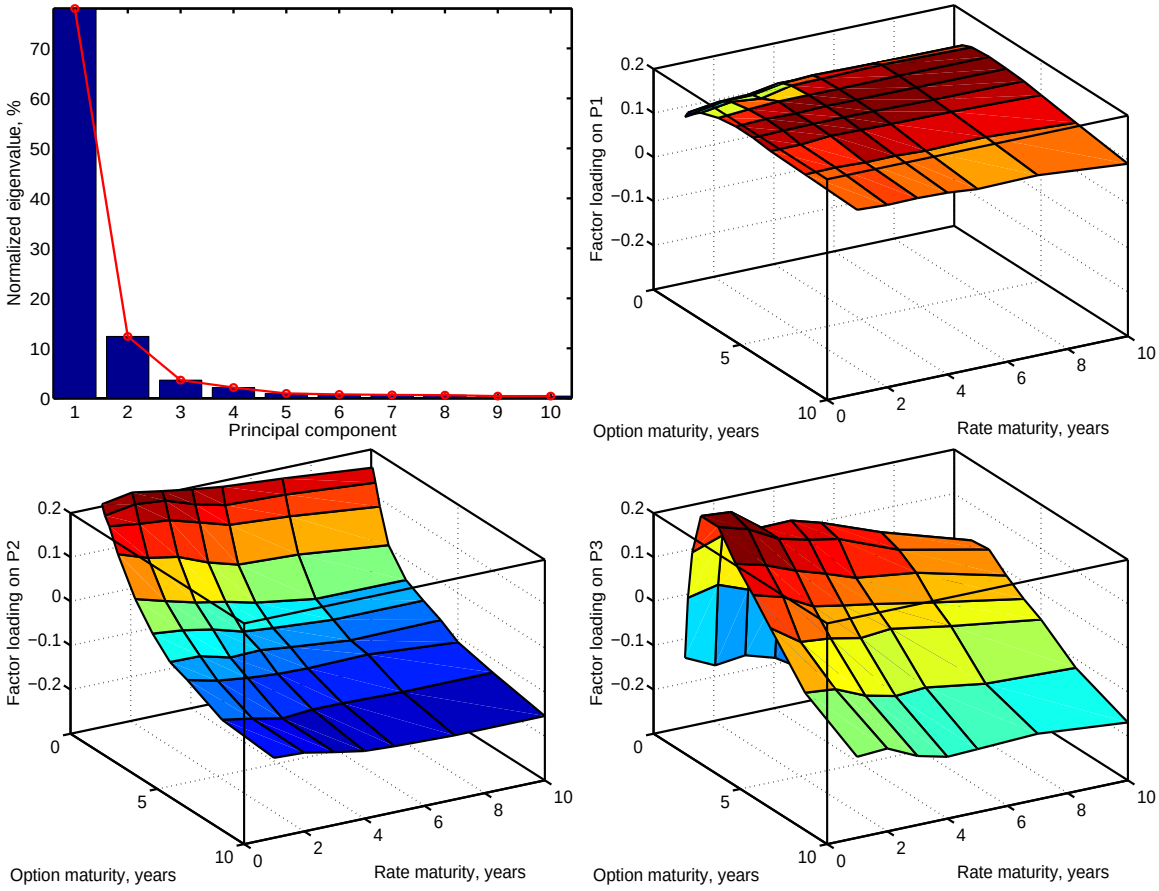

Figure 4

Principal component analysis on the implied volatility surface.

The bar chart in the first panel plots the first ten normalized eigenvalues of correlation matrix of the weekly differences on the 70 implied volatility time series, which can be interpreted as the percentage variation explained by each principal component. The remaining three panels plot the eigenvectors of the first three eigenvalues, respectively, which can be interpreted as the loading coefficients of the three principal components on the 70 time series along seven swap maturities and ten option maturities.

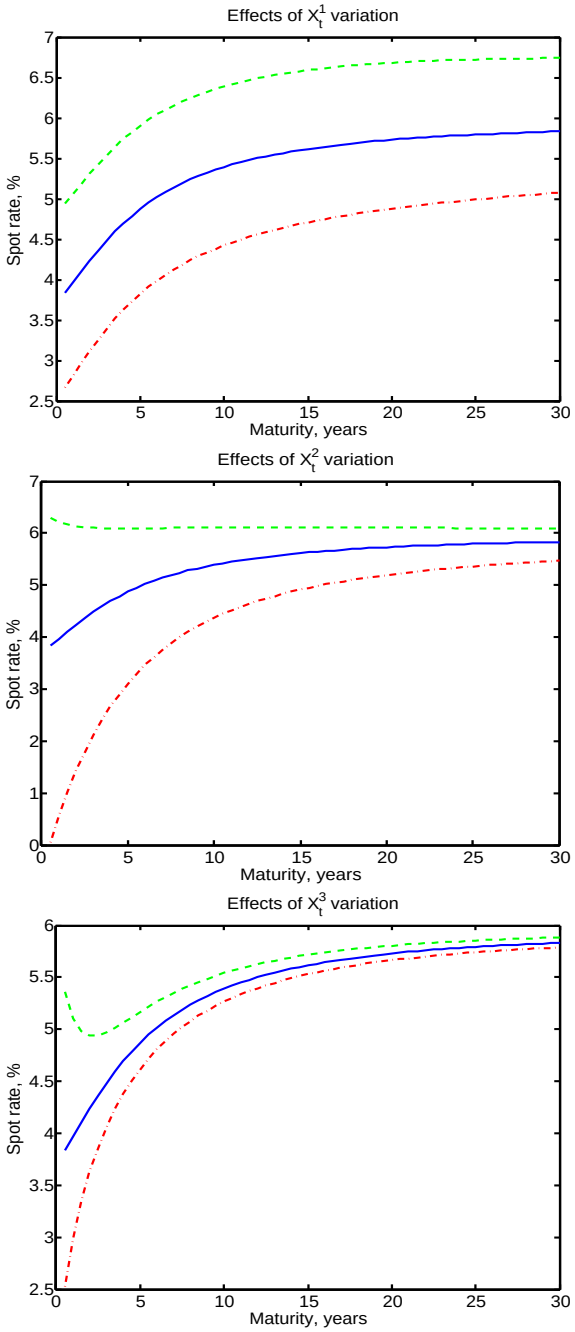

Figure 5

Interest rate factor shocks and yield curve responses.

The solid lines in each panel represent the continuously compounded interest rate term structure generated from the estimated three-factor model when evaluated at the sample averages of the extracted interest-rate factors. The dashed lines are obtained by setting one interest-rate factor to its 90-percentile while holding the other two to their average values. The dashed-dotted lines are obtained by setting one interest-rate factor to its 10-percentile while holding the other two to their average.

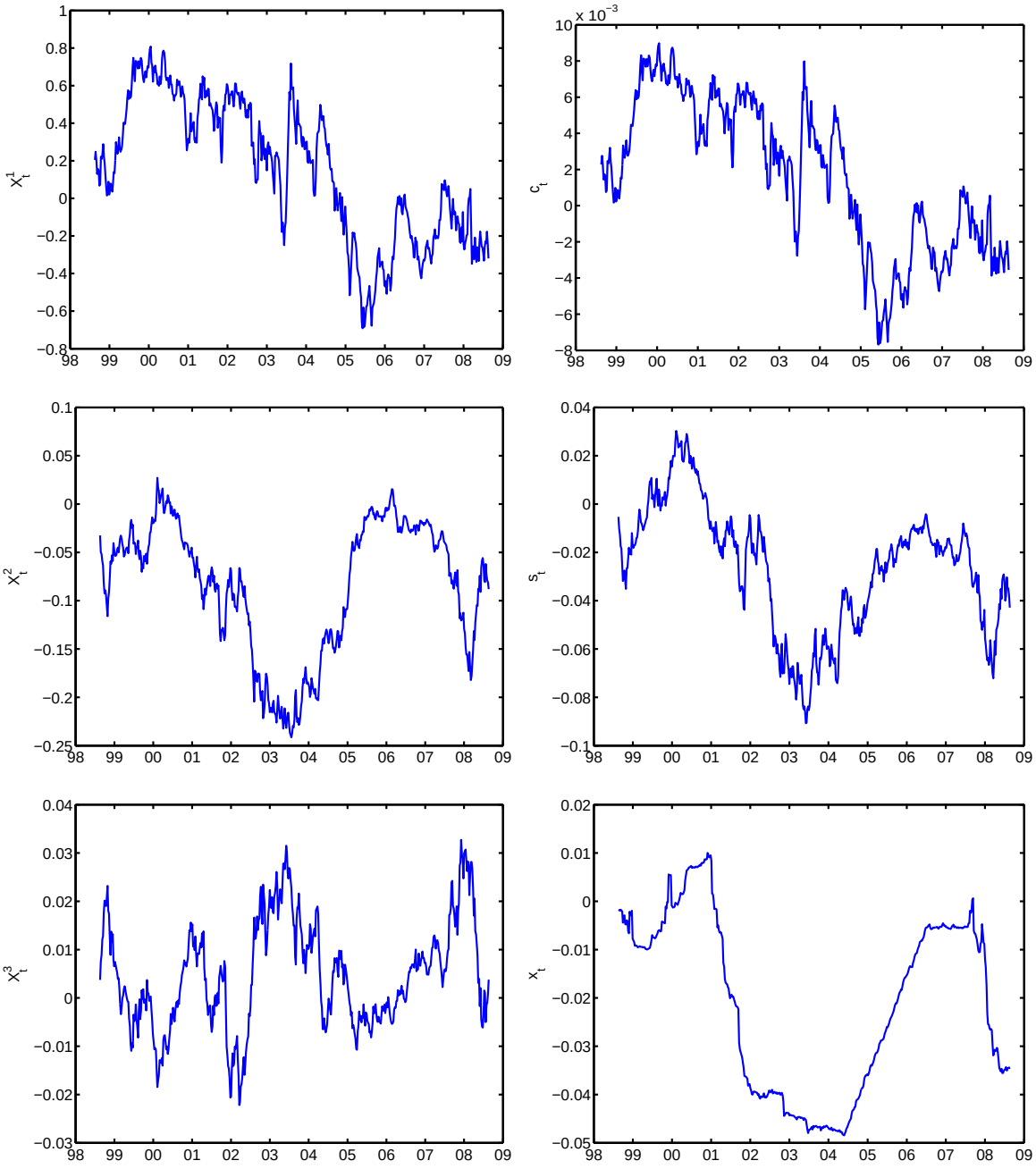

Figure 6

The time series of the interest-rate factors.

The time series of the three interest-rate factors are extracted using the unscented Kalman filter based on the first-stage estimated model parameters.

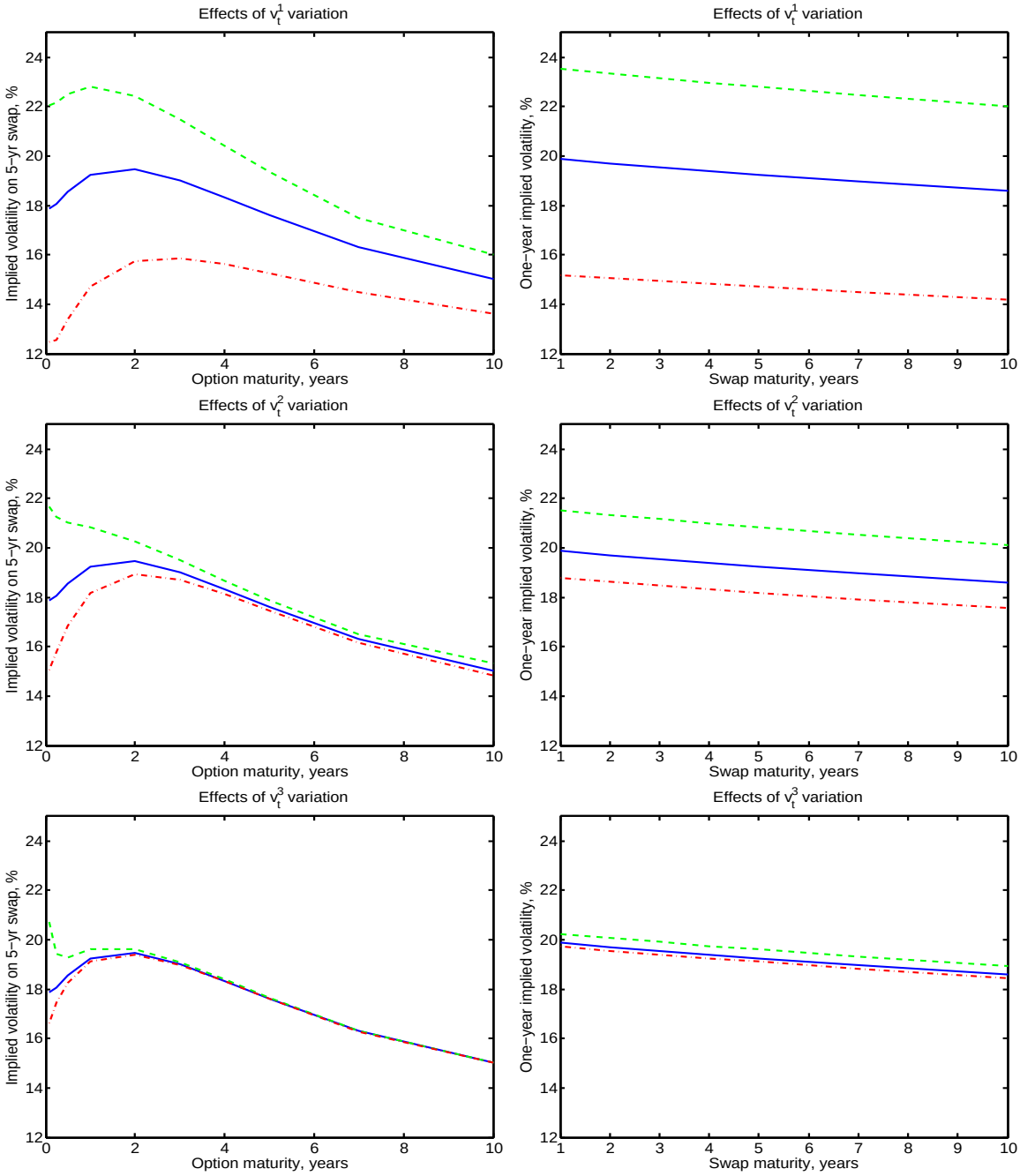

Figure 7

Volatility shocks and implied volatility responses under the $(3+3)$ model.

The solid lines in each panel represent the implied volatility generated from the estimated model when evaluated at the sample average of the volatility state variables. The dashed lines are obtained by setting one volatility factor to its 90-percentile while holding the other two to their average values. The dashed-dotted lines are obtained by setting one volatility factor to its 10-percentile while holding the other two to their average.

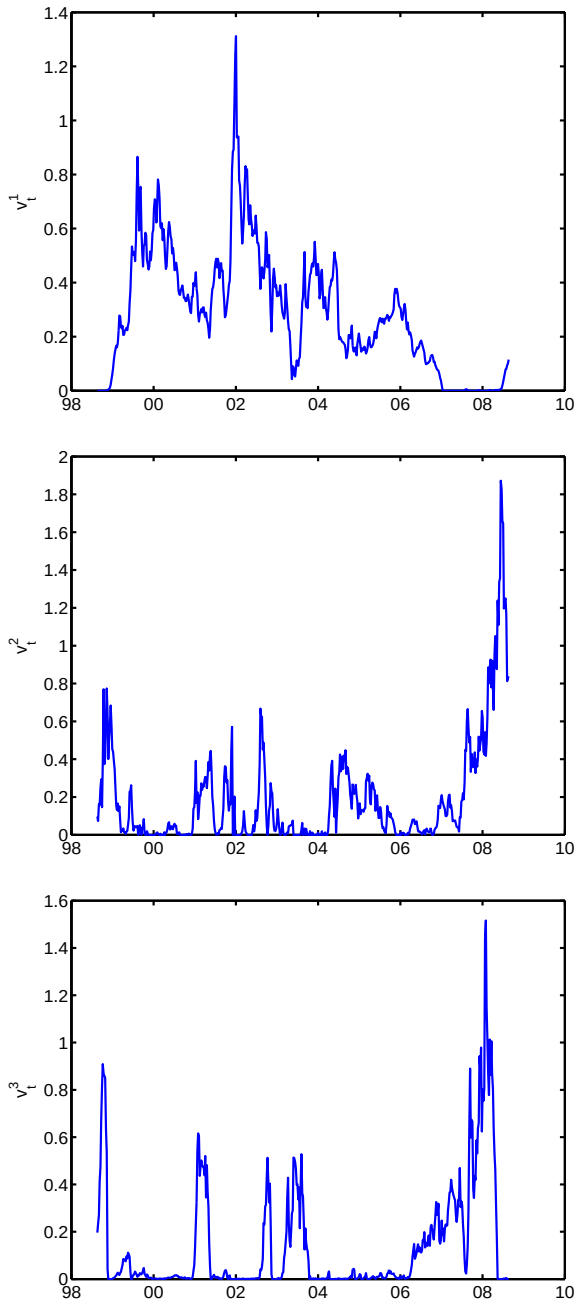

Figure 8

The time series of the interest-rate volatility factors.

The time series of the three interest-rate volatility factors are extracted from the estimated $(3+3)$ model.